ADVANCED BIOLOGY
www.advanced-bio.com

In Vitro Models of Blood and Lymphatic Vessels—Connecting Tissues and Immunity

*Amanda Bogseth, Ann Ramirez, Erik Vaughan, and Katharina Maisel**

Blood and lymphatic vessels are regulators of physiological processes, including oxygenation and fluid transport. Both vessels are ubiquitous throughout the body and are critical for sustaining tissue homeostasis. The complexity of each vessel's processes has limited the understanding of exactly how the vessels maintain their functions. Both vessels have been shown to be involved in the pathogenesis of many diseases, including cancer metastasis, and it is crucial to probe further specific mechanisms involved. In vitro models are developed to better understand blood and lymphatic physiological functions and their mechanisms. In this review, blood and lymphatic in vitro model systems, including 2D and 3D designs made using Transwells, microfluidic devices, organoid cultures, and various other methods, are described. Models studying endothelial cell-extracellular matrix interactions, endothelial barrier properties, transendothelial transport and cell migration, lymph/angiogenesis, vascular inflammation, and endothelial-cancer cell interactions are particularly focused. While the field has made significant progress in modeling and understanding lymphatic and blood vasculature, more models that include coculture of multiple cell types, complex extracellular matrix, and 3D morphologies, particularly for models mimicking disease states, will help further the understanding of the role of blood and lymphatic vasculature in health and disease.

1. Introduction

Blood and lymphatic vessels serve many purposes including circulating cells, oxygen, and other materials throughout the body, regulating transport of these materials into tissues, and modulating immunity. The development of in vitro models within the past two decades has allowed researchers to more effectively recapitulate and study the complex processes and functions of blood and lymphatic vessels. These processes include the cellular mechanisms involved in lymph/angiogenesis, material transport (oxygen, nutrients, etc.), and the role of blood and lymphatic vessels in tumor microenvironments and inflammation. Here, we discuss in vitro models that have used 2D and 3D designs to study and elucidate mechanisms relevant to blood and lymphatic vessel functions.

1.1. Introduction to Blood and Lymphatic Vessel Physiology

At the most fundamental level, blood vessels carry oxygen from the lungs to tissues and collect carbon dioxide from tissues for disposal through the lungs.[1] Lymphatic vessels drain interstitial fluid to maintain interstitial tissue pressure and fluid homeostasis.[2] Beyond these fundamental processes, blood and lymphatic vessels serve as routes for cellular and solute transport throughout the body, including immune cells, cancer cells, pathogens, and drugs.[3–8] Each vessel system has its own unique properties that allow transport, detailed below.

Blood vessels can be categorized into three different types: capillaries, veins, and arteries (**Figure 1**a). Capillaries are the smallest type embedded deep within tissues and are responsible for delivering oxygen and nutrients to each cell in the body. Capillaries consist of a single layer of endothelial cells which can be complete (uniform tight junctions), fenestrated (small pores), or sinusoidal (small pores and incomplete basement membrane). Arteries are larger blood vessels and are responsible for propelling oxygenated blood from the heart throughout the vasculature using the force provided by heart contractions. Veins are large blood vessels that carry deoxygenated blood from the tissues back to the heart. Both arteries and veins have one layer of endothelial cells, supported by a layer of smooth muscle cells, covered in a layer of collagen and elastic fibers. Hundreds of in vitro models of blood vessels exist that have studied basic principles of endothelial cell alignment due to shear flow and their behavior in complex diseases like inflammation and atherosclerosis.

Lymphatic vessels carry lymph, drained from interstitial tissue spaces, which contains excess plasma from blood, immune cells, antigens, and nutrients.[9] Transport occurs via diffusion, convection, and specialized intercellular junctions.[10] Two distinct vessel types are present in the lymphatic vasculature: initial and collecting vessels (Figure 1b).[11] The main difference between these vessels is the conformation of their intercellular junctions. Initial vessels have loose, button-like

A. Bogseth, A. Ramirez, E. Vaughan, K. Maisel
Fischell Department of Bioengineering
University of Maryland
College Park, MD 20742, USA
E-mail: maiselka@umd.edu

The ORCID identification number(s) for the author(s) of this article can be found under https://doi.org/10.1002/adbi.202200041.

DOI: 10.1002/adbi.202200041

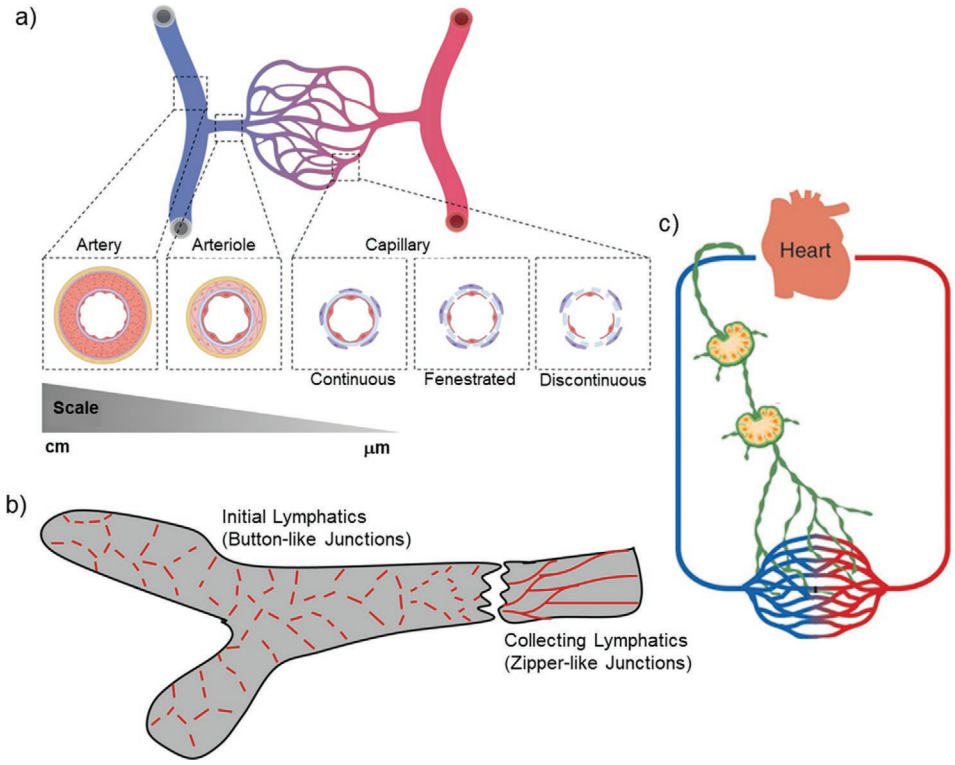

Figure 1. Anatomy of blood and lymphatic vessels. a) The differences between size and stroma coverage of arteries and capillaries. Reproduced with permission.[13] Copyright 2020, John Wiley and Sons. b) Lymphatic initial vessels are blunt-ended and have button-like junctions between endothelial cells. Collecting vessels contain valves and have zipper-like junctions between endothelial cells. Adapted with permission.[11] Copyright 2007, Rockefeller University Press. c) The capillaries of the blood and lymphatic systems are both embedded in tissues for oxygen supply and regulation of tissue pressure. Blood leaves the capillary network through the veins to become reoxygenated in the lungs. Lymph from the tissues travels from initial vessels to collecting vessels to lymph nodes, where the lymph is processed. Both systems merge at the subclavian vein that transports the fluid into systemic circulation. Reproduced with permission.[14] Copyright 2016, Wolters Kluwer Health, Inc.

tight junctions that allow the transport of solutes and fluid from the interstitial space into the lymphatic network. Lymph then flows from the initial vessels to the collecting vessels via pressure gradients (Figure 1c). Collecting vessels have continuous, zipper-like tight junctions to limit leakage of lymph as it travels throughout the vessels to lymph nodes. Collecting vessels also have valves, called lymphangions, that increase the propulsion of fluid throughout the vessels. Lymph nodes act as a reservoir for lymph where adaptive immune responses are formulated. Once the fluid has been filtered through the lymph nodes, it is transported to the subclavian vein to rejoin systemic circulation. Other than tissue homeostasis, the lymphatic vasculature is known to be involved in many physiological processes including lipid transport from the intestines, inflammation, and cancer metastasis.[12] Many of the mechanisms behind these processes are unknown due to the difficulty in studying lymphatic vessels in vivo. The recent progress in in vitro model development has elucidated important mechanisms of lymphatic biology and has been successful in modeling lymphangiogenesis and cancer-lymphatic interactions.

2. Introduction to In Vitro Models

In vitro models have been developed in 2D and 3D to mimic and study in vivo systems. Simple 2D models have been developed since the 1970s, and the advent of microfluidics has provided a large increase of more complex designs in recent years. In vitro models have been used to understand processes such as cellular organization, cell signaling effects, intercellular interactions, shear stress effects, and disease progression, to name a few. The models we discuss in this review focus on modeling endothelial cell-extracellular matrix interactions, endothelial permeability, multicellular tissue models, lymph/angiogenesis, and endothelial-cancer and endothelial-immune cell interactions.

2.1. 2D and 3D Models

2D in vitro models have been developed to aid in the understanding of biological questions, including how vessels respond to their extracellular matrices and regulate their junction barriers. 2D models are made with a monolayer of cells on a substrate, typically a Transwell. Despite the simplicity of these models, they have been imperative to understanding basic blood and lymphatic vessel biology. Several 2D models of blood and lymphatic vessels have been developed to study endothelial cell response to shear stress and the mechanisms of transport for various solutes such as albumin, dextran, and fatty acids (**Figure 2**).

3D in vitro models have been developed to more accurately recapitulate in vivo physiology. 3D models can include more

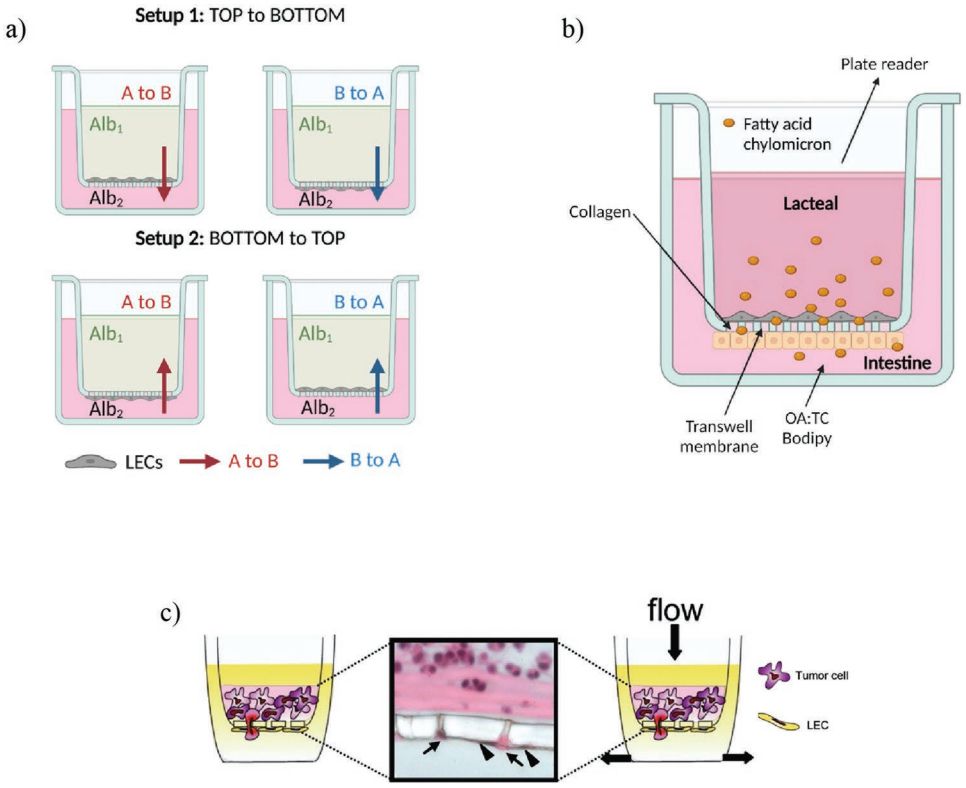

Figure 2. 2D Transwell models have been used for many applications, including studying transport with transmural flow, transport of fatty acids, and transendothelial migration of cancer cells. a) Simple Transwell model that has LECs on the top or bottom of the PET membrane and was used to test transmural flow effects on solute transport. Adapted with permission.[26] Copyright 2017, Wolters Kluwer Health, Inc. b) Simple Transwell model of intestinal transport, with LECs on the top layer and Caco-2 cells on the bottom layer, that was used to test fatty acid transport across the LEC layer. Adapted with permission.[27] Copyright 2009, John Wiley and Sons. c) Simple Transwell model of tumor cell transendothelial migration, with LECs on the bottom layer and cancer cells on the top layer of the membrane to test chemokine effects on migration. Reproduced with permission.[28] Copyright 2007, Elsevier.

complex parameters, including vascular lumens, natural or synthetic matrix materials that induce spontaneous lymph/angiogenesis, spheroid tumor models with multiple cell types, and inflammatory and diseased models (**Figure 3**). These models have been developed using various synthetic and natural extracellular matrices (ECM) which alter cellular behavior. Additionally, microfluidic devices made from polydimethylsiloxane (PDMS) have provided controllable micron-scale fluid flow which allows for real-time analyses of 3D vessel structures, cell junction permeability, and vessel perfusion.[15]

2.1.1. Endothelial Cell-ECM Interactions

Engineering blood and lymphatic vessels in vitro relies on the understanding of the interactions of endothelial cells with their biophysical environment. Due to the complexity of tissue organization in the body, it has taken lots of efforts to understand how the numerous biophysical components impact cellular organization and functions. Below, we summarize models that aim to understand the interactions of endothelial cells with their ECM (**Table 1**).

A recent study by Shin et al. tested how ECM morphology affects blood endothelial cell alignment and monolayer formation in 2D. They used a microgroove-patterned nanofiber platform, fabricated using a femtosecond laser.[16] They tested blood endothelial cell (BEC) alignment on four different platforms, including random alignment of nanofibers, aligned nanofibers, and two microgroove-patterned nanofibers with either a 20 or 80 µm distance between grooves. They seeded BECs on these platforms and assessed alignment and resistance of the cells, which are important characteristics of a healthy blood vessel endothelium. They found that BECs were able to detect the micropattern and change their behavior. On day 1 after seeding, BECs were more elongated on the 20 µm compared to the 80 µm microgroove-pattern, which also resulted in a smaller cell body aspect ratio for the 20 µm compared to the 80 µm pattern. On day 3 after seeding, they found that monolayer formation and alignment were similar between BECs cultured on microgroove-pattern nanofibers and the aligned nanofiber controls, indicating that the cells were able to align on the microgroove-pattern nanofibers as efficiently as the optimal control. To test the monolayer resistance, they assessed monocyte adhesion to mimic the accumulation of blood components in the vessel, which occurs in diseased states such as atherosclerosis. They found that the BECs on the 20 µm microgroove-pattern nanofibers had lower monocyte adhesion in normal and inflammatory conditions compared to the random and aligned

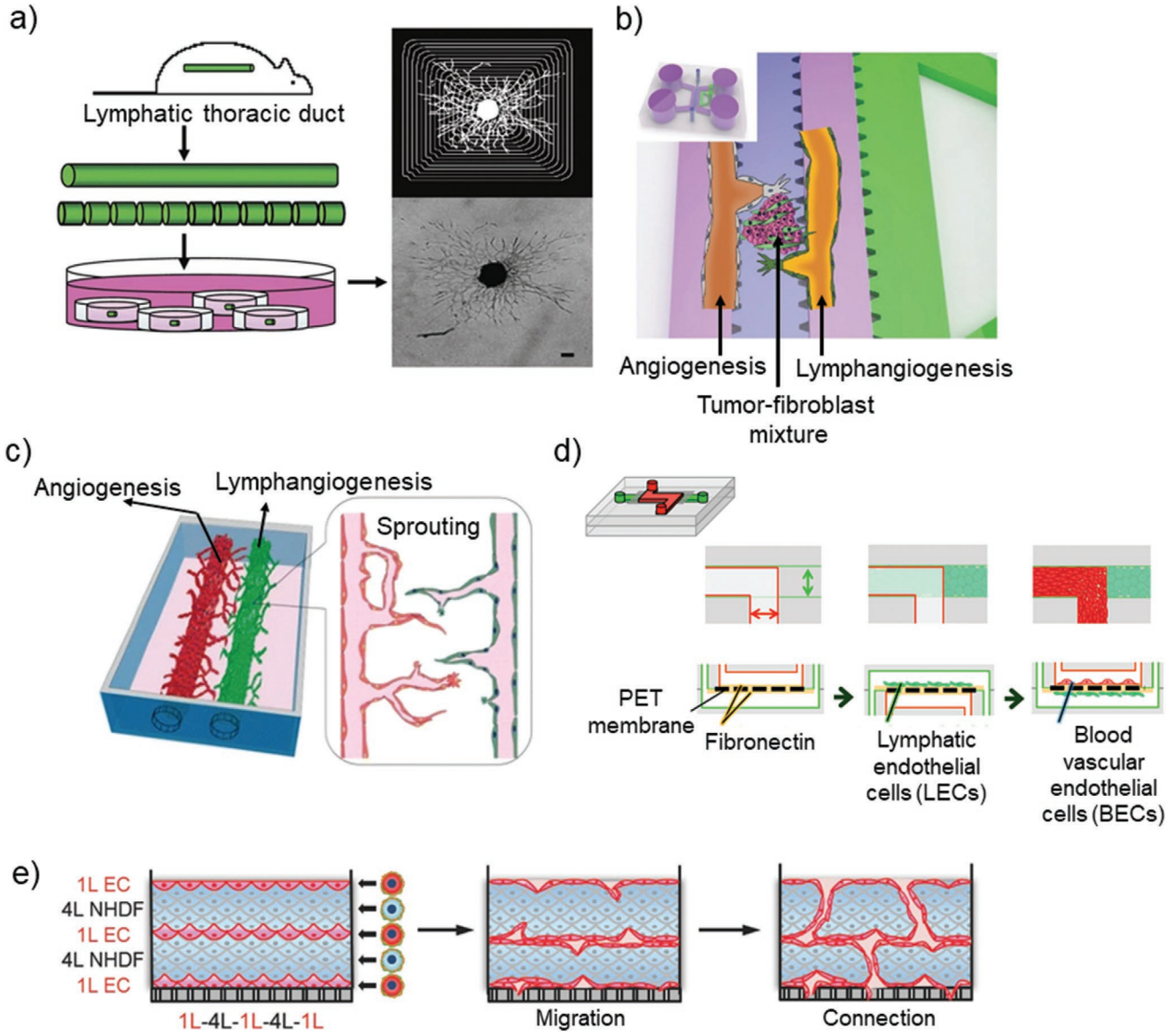

Figure 3. 3D models with lymphatic vessels have been made several different ways and have been used to model lymphangiogenesis, tumor interactions, and perfusion. a) A ring duct model was the earliest 3D model reported for lymphangiogenesis. Reproduced with permission.[51] Copyright 2008, Springer Nature. b) A 3D microfluidic model with BECs and LECs seeded in vessel channels were tested for sprouting towards a tumor-fibroblast cell mixture to determine how cancer induces lymphangiogenesis and angiogenesis. Reproduced with permission.[56] Copyright 2017, John Wiley and Sons. c) An acrylic plate with collagen-coated vessel channels was created to test growth factor stimulation of angiogenesis and lymphangiogenesis in 3D. Reproduced with permission.[52] Copyright 2018, Springer Nature.) d) A 3D microfluidic device was made from PDMS to seed both BECs and LECs on a PET membrane to test the permeability effects of dextran and LY during healthy and inflammatory conditions. Reproduced with permission.[37] Under creative commons license. e) A cell layering technique created a 3D matrix of fibroblasts and LECs and BECs to test perfusion throughout the vessel network. Reproduced with permission.[57] Copyright 2016, John Wiley and Sons.

nanofiber controls. This lower monocyte adhesion was found to be caused by the decreased expression of the monocyte adhesion related markers E-selectin, C-C Motif Chemokine Ligand 2 (CCL2), and vascular cell adhesion molecule-1 (VCAM-1). Overall, they found that the microgroove-patterned nanofibers resulted in more elongated and aligned monolayers which led to lower monocyte adherence, indicating higher resistance for the BEC monolayer.

Endothelial cell-ECM interactions can also be studied using materials found in vivo. Altering ECM composition in vitro has shown to alter vessel stability, organization, and junction barrier tightness. For example, Ng et al. created a 0.35% v/v concentrated collagen matrix with 50 ng mL^{-1} phorbol 12-myristate 13-acetate (PMA) and seeded LECs and BECs within the 3D matrix.[17] They found that interstitial flow induced tube-like vessel structures, observed by extensions of F-actin toward neighboring cells, and extensions of filopodia attached to the matrix. LECs and BECs were also found to align parallel to the direction of flow when compared to static conditions. They concluded that this was indicative of lymphangiogenesis and angiogenesis.

Table 1. Summary of in vitro models that studied fundamental topics of blood and lymphatic vessels.

Author, year	Cell type	Model material/type	Dimension	Physiological process modeled
Shin et al., 2017.	HUVECs	Poly(L-lactide) PLLA nanofibers coated with human plasma fibronectin (20 μg mL^{-1})	2D	Anisotropic architecture of blood endothelium
Ng et al., 2004	Human neonatal foreskin LECs and BECs	Gel of 0.35% v/v rat tail type I collagen and phorbol 12-myristate 13-acetate (50 ng mL^{-1})	3D	Interstitial flow and ECM effects on BEC and LEC vessel formation
Helm et al., 2006	Human dermal LECs and BECs	Porous polyethylene coated with various concentrations of fibrinogen and collagen	3D	Fibrinogen and collagen concentration effects on BEC and LEC vessel formation
Bonvin et al., 2009	Human dermal LECs and BECs	PDMS coated with fibrinogen (3 mg mL^{-1})	3D	Interstitial flow and VEGF effects on BEC and LEC vessel formation
Chan et al., 2013	Human dermal LECs and BECs	PDMS coated with rat tail type I collagen (8 mg mL^{-1})	3D	Collagen crosslinking effects on BEC and LEC vessel formation
Henderson et al., 2021	Human dermal LECs and BECs	PDMS coated with various concentrations of collagen and fibronectin	3D	Collagen and fibronectin concentration effects on LEC intercellular junctions
Breslin et al., 2009	Adult human dermal LECs and BECs	Gold electrodes on culture plates coated with gelatin (unknown concentration)	2D	Shear stress effects on LEC barrier function
Triacca et al., 2017	Human neonatal foreskin LECs	Transwells coated with collagen (unknown concentration)	2D	Solute transport mechanisms across LEC layer
Dixon et al., 2009	Human neonatal foreskin LECs	Transwells coated with rat tail type I collagen (50 μg mL^{-1})	2D	Lipid transport across LEC layer
Reed et al., 2014	Human neonatal dermal LECs	Transwells coated with rat tail type I collagen (100 μg mL^{-1})	2D	Mechanism of lipid transport across LEC layer
Price et al., 2008	Human dermal LECs	PDMS coated with rat tail type I collagen (10 mg mL^{-1})	3D	cAMP effects on LEC barrier function
Thompson et al., 2017	Human dermal LECs	PDMS coated with rat tail type I collagen (7 mg mL^{-1})	3D	Transport across lymphatic vessels
Sato et al., 2015	Human dermal LECs and BECs	Porous polyethylene terephthalate (PET) membrane coated with fibronectin (0.1 mg mL^{-1})	3D	Permeability of LECs and BECs

Another example was reported by Helm et al. who tested the effects of ECM density on LEC and BEC stability with interstitial flow.[18] They embedded the cells in four 3D matrices made of different concentrations of collagen and fibrinogen, inserted them into a cylindrical tube made of porous polyethylene, and assessed cellular organization. They found that BECs organized better in a higher collagen concentration (1:1 ratio of collagen:fibrinogen vs 1:2 ratio), and LECs organized best in fibrinogen-only matrices. Addition of interstitial flow was found to induce more cellular organization, as observed via a high number of multicellular structures. This study highlighted that different ECM compositions are optimal for different cell types.

Building off of this model, Bonvin et al. developed a nine-plate microfluidic device that can test nine different experimental conditions at one time, confirmed through fluorescent dye testing for leakage between chambers.[19] They tested the effects of interstitial flow with vascular endothelial growth factor (VEGF) stimulations. The cellular effects of interstitial flow and VEGF were similar to their previously tested single device, confirming the validity and control for their nine-chamber model. The best models of LEC organization were created with VEGF stimulation (100 ng mL^{-1}) and interstitial flow presence (1–2 μm s^{-1}). Overall, this platform allowed for researchers to study multiple parameters at once and determine optimal conditions for LEC organization that can be used for subsequent studies.

Crosslinking the ECM material has been shown to affect the stability of endothelial cells, as reported by Chan et al..[20] The authors created a 3D microfluidic model made of PDMS and a needle-punched lumen. They added collagen gels crosslinked with genipin or 1-ethyl-3-(3-dimethylaminopropyl), and seeded LECs or BECs within the lumen. They found that the LECs and BECs were more stable with either of these crosslinking treatments compared to no crosslinking. They found more delamination of both cell types when destabilizing flow was introduced in non-crosslinked models compared to the crosslinked models. This increased stability was due to the change in elastic modulus. Overall, they showed that the crosslinking treatments are useful when creating stable in vitro vessel models of both LECs and BECs.

A more recent study reported by Henderson et al. demonstrated the importance of ECM material on tight junction permeability.[21] Using a 3D microfluidic model made from PDMS with a needle-punched lumen, they seeded LECs on a collagen-only matrix, or a collagen and fibronectin matrix. Through staining of the tight junction protein VE-cadherin, they found that fibronectin tightens LEC junctions through the activation of integrin $\alpha 5$. This study was one of the only results that showed ECM material by itself can alter LEC junction barriers. Future work in this area can help determine the differences between initial and collecting vessels, which have drastically different roles in vivo.

These models have studied the ways to recapitulate vessels in vitro. When making new vessel models, it is important to understand the effects that matrix stiffness has on vessel formation, which is shown to be tailored by crosslinking collagen gels, using specific concentrations and mixtures of ECM

proteins, and stimulating cells with specific growth factors. In future models, it could be beneficial to use an ECM composition that is found in the specific physiological mechanism in the in vitro model. For example, if one is studying cancer-mediated interactions of tumor metastasis, the ECM of the vessels in a model should replicate what is found in vivo. Another example includes studying intercellular junctions of LECs, and noting whether the junctions replicate initial or collecting junctions.

2.1.2. Modeling Transendothelial Transport in Blood and Lymphatic Vessels

Blood vessels are crucial for the mass transport of key molecules and fluids throughout the body. Understanding how blood vessels coordinate transport throughout a system is key to getting a better understanding of how these vessels may respond to different conditions and stimuli. Researchers have studied the mechanisms of transport into and through blood vessels, how different disease states affect transport, and how different therapeutics may affect transport. For more details, we refer the readers to several excellent reviews on models of transport across blood vessels.[22–25]

Transport of solutes from interstitial fluid into lymphatic vessels is a critical process to maintain homeostasis. Interstitial flow is present throughout all tissues and can change in different disease states.[29] Understanding the impact of interstitial flow on LECs can provide context for many physiological processes. An early model that studied the effects of interstitial flow on LECs was reported by Breslin et al..[30] They used a gold electrode plate to culture LECs in a 2D monolayer and assessed their barrier function via transendothelial electrical resistance (TEER) when exposed to interstitial flow. They found that shear stress increases barrier function, which is dependent on the actin cytoskeleton and Ras-related C3 botulinum toxin substrate 1 (Rac1) protein interactions between cells. These studies showed that LECs respond to interstitial flow in vitro, emphasizing the importance of including this stimulus to accurately reconstruct the physiology in vivo.

Since lymphatic transport of solutes across the endothelial barrier is necessary to maintain homeostasis, it is important to understand the mechanisms that allow solutes to pass through the lymphatic vessel wall. In vivo models have fallen short in understanding these mechanisms due to the inability to observe transport in real-time. A recent in vitro model reported by Triacca et al. used a 2D Transwell model to study the route of dextran and albumin transport across a LEC monolayer (Figure 2a).[26] By seeding the LECs either on the top or bottom of the Transwell insert, they found that the albumin transport was directional, with higher transport occurring from the basolateral to apical direction. This mimics the transport from the interstitial space to vessel lumen found in vivo. Their study also demonstrated that transendothelial permeability is primarily achieved through the transcellular pathways of vesicle formation and transcytosis, especially in the presence of transendothelial flow (simulating interstitial flow). When they treated the cells with inflammatory cytokine tumor necrosis factor (TNF-α), they observed an increase in transcellular transport. This model effectively showed the routes of transport over the endothelium and showed how physiological states like transmural flow and inflammation affected the transport.

A specialized transport function of initial lymphatic vessels occurs in the intestines, where lymphatic vessels take up lipids, in the form of chylomicrons, from the intestines and deliver them to systemic circulation.[31] Enterocytes in the intestines collect lipids and package them into chylomicrons, small lipid particulates, that are then released at the basolateral side of the epithelium where they are drained via initial lymphatics, or lacteals.[32] Disrupted uptake of lipids by the lymphatics has been linked to diseases such as obesity.[33] The specific mechanisms of how these lipids are transported across the lymphatic endothelium are not well understood. Two 2D in vitro models were developed using Transwells to study the mechanisms of transport for chylomicrons. Dixon et al. differentiated Caco-2 cells into their enterocyte phenotype, seeded them on the basal side of the Transwell, and seeded LECs on the apical side (Figure 2b).[27] By testing the transport of fluorescent Bodipy-linked fatty acid, they found that most transport was primarily mediated by transcellular pathways in a physiologically relevant polarized direction rather than the paracellular pathway, although both pathways were present. A follow-up study by Reed et al. tested LEC transport of dextran and Bodipy-linked fatty acid across a monolayer of LECs on the apical side of a Transwell.[34] While Caco-2 cells were not present in the model, Caco-2 lipid secretions were tested for transport. They found that the apical transcytosis of fatty acids was dependent on ATP. When they tested transport with Caco-2 lipid secretions, they found the transport was even more dependent on ATP, as demonstrated by the lower amounts of transport with higher concentrations of ATP inhibitor. Since the Caco-2 lipid secretions were larger in size compared to the Bodipy-linked fatty acids, they hypothesized that the increased ATP dependence for Caco-2 lipid secretions was likely due to the lower ability for paracellular transport to occur. Overall, these findings are important to understand the basic physiology of lymphatics, particularly in the gut, and can be used to design drugs that target these mechanisms of transport for diseases that alter lipid uptake.

A number of 3D models have also emerged that can model transport in and out of a full lumen instead of a 2D monolayer. The earliest 3D model of barrier function was reported by Price et al. who created lymphatic vessels on a collagen gel in a silicone elastomer (Figure 3a).[35] The cells in this gel created lymphatic lumens that were tested for barrier integrity. They found that cAMP increased the integrity observed through decreased permeability coefficients of albumin and dextran, and increased VE-cadherin in the junctional stain. With activation of cAMP using 80 μM of dibutyryl cAMP, the permeability coefficients of transport of 10kDa dextran across LECs decreased from 1.7×10^{-6} to 6.2×10^{-7} cm s^{-1}. Thus, they concluded that cAMP is an important intracellular regulator for lymphatic barrier function, which is a similar result of cAMP regulation in blood vessels.

Another model was reported by Thompson et al. who created a 3D microfluidic device out of PDMS with needle-punched drainage channels coated with collagen to mimic the relationship between the interstitial space and lymphatic vessels.[36] They tested rates of fluid and solute removal from the collagen gel into the lymphatic drainage channel with and without the

presence of LECs. They found that fluid drainage into the channels was not affected by the presence of LECs. However, with LECs present, the solute drainage of albumin and dextran was enhanced. Their model showed an example of how to incorporate the lymphatic vessels into a tissue-engineered model to make it more physiologically relevant.

Another 3D microfluidic model was reported by Sato et al. which consisted of a blood vessel on top of a lymphatic vessel separated by a polyester (PET) membrane (Figure 3d).[37] They studied the permeability of lucifer yellow (LY) and dextran through each vessel type with pulsating luminal flow and inflammatory stimulation. They observed that the permeability of LY and dextran decreased with pulsating flow, indicating that the pulsating flow resulted in tighter intercellular junctions in both vessel types. When inflammation was mimicked using histamine stimulation, intercellular junctions were destabilized, observed through intracellular localization of VE-cadherin and claudin-5, and the permeability of LY and dextran increased in both vessel types. This model effectively demonstrated the use of both blood and lymphatic vessels in one model and how permeability can be modulated using flow and inflammatory factors.

Overall, these models have reported findings of how transendothelial transport is modulated by interstitial flow and inflammatory factors. In the future, more relevant models that study a specific disease could benefit the progress of understanding how transport is modulated in certain diseases, and what factors of lymphatic biology can be targeted by drugs.

2.1.3. Modeling Angiogenesis and Lymphangiogenesis

New growth of blood and lymphatic vessels from pre-existing vessels is termed angiogenesis and lymphangiogenesis, respectively.[38] During fetal development, nearly all blood vessels develop in this manner following the growth of the first BEC-lined lumen.[39] Similarly, the establishment of lymphatic sacs during fetal development induces the development of lymphatic vessels via lymphangiogenesis, although this process happens in much later stages of development compared to blood vessels.[39] These processes are highly regulated by interactions with neighboring cells and extracellular factors.

VEGF signaling is used in the body to induce both processes. Lymphangiogenesis is mainly regulated by VEGF-C and its receptor VEGFR-3[40] Angiogenesis is mainly regulated by VEGF-A and its receptors VEGFR-1 and VEGFR-2.[41] Both processes are highly active during development, but they slow down once an adult organism has formed. In disease, a lymph/angiogenic switch occurs via an overdose of proangiogenic signals, and the process of new vessel development begins because of the increased signals. This occurs for both angiogenesis and lymphangiogenesis in cancer, inflammation, and wound healing.[42–44] Therefore, understanding the specific interactions between endothelial cells and their surrounding environment is imperative for understanding development or progression of diseases, and how vessels aid in wound healing (**Table 2**).

Models of Angiogenesis: Hundreds of models of angiogenesis have been reported in the literature, and a few will be discussed here. Additionally, we recommend articles by Vailhe et al.[45] and Morin et al.[46] for a full overview.

Angiogenesis is dependent on mechanical properties of the microenvironment, which are actively altered in diseased states. Natividad-Diaz et al. studied 3D matrix stiffness and angiogenesis.[47] The group encapsulated induced pluripotent stem cell (iPSC)-derived BECs in a hyaluronic acid (HA) hydrogel and measured vasoactivity and vessel growth across different matrix stiffnesses. Matrices with a higher shear modulus induced a stable tube formation and longer vessel formation in an angiogenesis assay. Additionally, the formation of the stable tube corresponded with an increase in nitric oxide (NO) production, indicating functional BECs. Less stiff matrices initially

Table 2. Summary of angiogenesis and lymphangiogenesis in vitro models.

Author, year	Cell type	Model material	Dimension	Physiological process modeled
Natividad-Diaz et al., 2019	Human induced pluripotent stem cell derived endothelial cells	Hydrogel	3D	Angiogenesis and nitric oxide production
Davidov et al., 2020	HUVECs	Hydrogel with porcine arterial extracellular matrix	3D	Angiogenesis
Lee et al., 2020	Primary human brain microvascular endothelial cells, HUVECs, and primary human pericytes	Bovine plasma fibrin hydrogel (10 mg mL^{-1}) with fibrin (2.5 mg mL^{-1}) for cell seeding	3D	Angiogenesis with perivascular cells
Pauty et al., 2018	HUVECs	PDMS with porcine tendon Type I-A collagen (3 mg mL^{-1})	3D	Angiogeneisis
Bruyere et al. 2008	Mouse thoracic ducts	Agarose solution type VII (25 mL per 100 mm culture dish) with rat tail type 1 collagen (2 mg mL^{-1})	3D	Lymphangiogenesis
Osaki et al., 2018	HUVEC and human neonatal dermal LECs	Acrylic chamber coated with rat tail type I collagen (2.4 mg mL^{-1})	3D	Lymphangiogenesis
Gibot et al., 2016	Human neonatal foreskin derived LECs and BECs	Stacks of dermal fibroblast sheets in tissue plates	3D	Lymphangiogenesis
Kim et al., 2016	Human dermal BECs	PDMS coated with fibrin (2.5 mg mL^{-1})	3D	Lymphangiogenesis
Landau et al., 2021	Human LECs, human adipose microvascular endothelial cells, neonatal normal human dermal fibroblasts	CelGro collagen scaffold	3D	Lymphangiogenesis

had sprouting, but were unable to form mature tubes or release sufficient NO. Decellularized native ECMs provided bioactivity, yet lacked reproducibility and are challenging to isolate one parameter compared to synthetic biomaterials.

Davidov et al. recognized the importance of supporting cells, along with the ECM, in angiogenesis.[48] The group used porcine arterial ECM (paECM) and turned it into a hydrogel to be used in culturing BECs in a 3D environment. Supporting cells, including smooth muscle cells and mesenchymal stem cells, were added to the culture to determine their effects on angiogenesis. It was found that the addition of smooth muscle cells in a 2:1 ratio formed clusters and outgrew the BECs, while mesenchymal stem cells in a 2:1 ratio helped create a complex network structure. They compared BEC apoptosis on the paECM hydrogel with alginate and Matrigel controls and found almost no apoptosis on the paECM hydrogel. Additionally, they validated their model using known angiogenic factors, VEGF and basic fibroblast growth factor (bFGF). They found that while bFGF alone could induce proliferation and sprouting, the combination of VEGF and bFGF produced a higher number of migrating and sprouting cells.

It has recently been shown that pericytes play a large role in angiogenesis by stabilizing and helping mature newly formed vessels. Lee et al. developed a 3D microfluidic coculture system that housed a lumen lined with BECs and pericytes, surrounded by a collagen gel.[49] Angiogenesis was induced in their system using VEGF-A. They found that while the addition of pericytes prevented expansion of the original vessel, it did enhance sprouting and elongation of newly formed vessels. The newly formed vessels in this coculture model were longer and more tightly bound compared to BEC monocultures. They also observed that pericytes covered the basal side of both the original vessel and any newly formed sprouts. Therefore, they showed that including pericytes in the in vitro model enhanced angiogenesis and vessel function

In addition, Pauty et al. developed an 3D in vitro model to study angiogenesis using a microvessel-on-a-chip platform.[50] The group developed a PDMS-based chip that housed blood microvessels that were supported by a collagen matrix. They added VEGF-A to study the initial steps of angiogenesis. They found that initial sprouting occurred at day 4 of culture, distinguishable sprouting occurred at day 6, and further growth occurred until the end of the experiment at day 10. They also tested two angiogenesis inhibitors in their model, sorafenib and sunitinib, which target the VEGF-A receptor VEGFR-2 on their model. These inhibitors caused a decrease in sprouting from the original microvessel, showing that these receptors are critical for angiogenesis. This model can be used to test drugs to determine at what stage of angiogenesis the drug inhibits the process.

As shown through this brief description of models, many characteristics of angiogenesis are still being discovered and modeled in vitro. These studies on effects of matrix stiffness, using more biologically relevant models using biological ECM (e.g., paECM) and supporting cells (e.g., smooth muscle cells and pericytes), and the ability to track angiogenesis stages in vitro have provided progress in the field. Overall, these in vitro models were able to show that VEGF-A and receptors VEGFR-1 and VEGFR-2 were regulators of angiogenesis. Further progress can be made when using these characteristics to make specific physiological models of certain processes.

Models of Lymphangiogenesis: Over the last 14 years, the development of lymphangiogenic in vitro models has shown the importance of VEGF-C and platelet-derived growth factor BB (PDGF-BB) signaling in lymphatic sprouting, and matrix metalloproteinases (MMP) in matrix remodeling. These models have been developed using several materials including collagen matrices, acrylic vessel lumens, CelGro scaffolds, microfluidic devices, and cell layering.

In 2008, Bruyere et al. reported the first in vitro model of lymphangiogenesis using a ring assay of LECs from a mouse thoracic duct in a 3D collagen matrix.[51] From their study, they concluded that VEGF-C induced VEGFR3-mediated lymphatic sprouting, the growth factor PDGF-BB enhanced its receptor, platelet-derived growth factor receptor β (PDGFR-β), which mediated vessel formation, and MMP-2 stimulated lymphatic sprouting. These findings have subsequently been reproduced in various other models. As reported in a blood vessel and lymphatic vessel model created by Osaki et al. in 2018, lymphangiogenesis and angiogenesis were stimulated by VEGF-C through the VEGFR-3 and VEGFR-1 receptors, respectively (Figure 3c).[52] The main MMPs secreted from the cells were MMP-2 and MMP-9 and led to sprouting of lymphatic and blood vessels. Osaki et al.'s more complex model looked at the response to stimulation factors and the interactions between blood and lymphatic vessels, which better recapitulated the physiology in vivo compared to earlier models.

For a more in-depth look into how VEGF-C induced lymphangiogenesis, Gibot et al. created a 3D model with fibroblast-derived ECM and LECs and determined that induction of extracellular signal-regulated kinase 1/2 (ERK1/2) signaling was responsible for the VEGF-C and hepatocyte growth factor (HGF)-induced lymphatic sprouting.[53] Kim et al. found similar results in their lymphatic vessel model made from PDMS, with one central channel and two side channels seeded with stromal fibroblasts.[54] They incorporated interstitial flow and growth factors including VEGF-A, C, and D, bFGF, sphingosine 1-phosphate (S1P), HGF, insulin-like growth factor (IGF1), and PDGF-BB, and showed that higher interstitial flow, along with these growth factors, enhanced lymphatic sprouting. They observed that interstitial flow induced ERK1/2 phosphorylation that led to enhanced sprouting, similar to what was found in other studies.

Even more recently, Landau et al. reported the prolymphangiogenic effects of culturing LECs with dental pulp stem cells.[55] They found through knock down of PDGFR-β that vessel formation was inhibited. Thus, PDGFR-β mediates PDGF-BB-induced vessel formation. They further looked at the effect of cyclic stretch on vessel outgrowth in their 3D model and found that vessel formation was only present in the depths on the scaffold, not on the surface. This effect was dependent on proteins that are associated with cell motility, the cytoskeleton, membrane organization, and cell polarity. Lastly, this scaffold was successfully implanted in vivo to promote lymphangiogenesis for wound healing.

Overall, these in vitro models have validated and discovered gene-level drivers of lymphangiogenesis that include VEGF-C and VEGFR-3 signaling, PDGFR-β and PDGFR-BB signaling, MMP-2 and MMP-9 signaling, and ERK1/2-induced lymphatic sprouting, which has also been found in vivo. Despite these

findings, lymphangiogenesis in disease is still not well understood, and disease-focused models of lymphangiogenesis need to be developed.

3. Models of Endothelial Cells in Inflammatory Diseases

Endothelial cells have been shown to have vital roles in mediating and reducing inflammatory conditions. This has been shown in part due to the development of novel in vitro model systems that allow probing of specific disease or immune-endothelial cell interactions. Here, we describe model systems that have been developed to study the role of blood and lymphatic vessels in the development of cancer and vascular inflammation.

3.1. Tumor-Blood Vessel Interactions

Many in vitro models have focused on the intricate effects of the tumor microenvironment on blood vessels (**Table 3**). Many primary tumors alter their microenvironment mechanically through increased vessel leakage, increased interstitial pressure, and a discontinuous endothelial barrier.[58] These mechanical changes, termed the enhanced permeation and retention (EPR) effect, may help promote vascularization of the tumor, promote immune tolerance, and encourage metastasis and cancer cell migration.[58,59] Cancer cells have numerous effects on nearby blood vessels that may be used in future drug delivery strategies. Tang et al. used a microfluidic device with tumor and vascular compartments to demonstrate the effect of cancer cells on blood vessel permeability.[60] The vessel displayed increased permeability when cocultured with metastatic breast cancer cells or tumor-primed media, suggesting a biochemical signaling from cancer cells to endothelial cells. Enhanced permeability was most significant with metastatic breast cancer cells. The group noted increased extravasation of liposomal carriers when cocultured with metastatic breast cancer cells as well. This device has the potential to be used in drug screening.

Angiogenesis is a critical part in cancer spreading and more insights into understanding the role of angiogenesis in cancer can be used to better manage cancer. Previous treatments have included delivering angiogenesis inhibitors to cancer patients, but these treatments are typically insufficient because other mechanisms, such as neo-vasculogenesis, vascular mimicry,

Table 3. Summary of tumor-blood vessel in vitro models.

Author, year	Cell type	Model material	Dimension	Physiological process modeled
Tang et al., 2017	Primary human breast tumor associated endothelial cells, MDA-MB-231, and MCF-7	PDMS coated with fibronectin and gelatin	3D	Enhanced permeation and retention (EPR) effect on blood vessels
Buchanan et al., 2014	Telomerase-immortalized human microvascular endothelial cells and MDA-MB-231	PDMS coated with rat tail Type I collagen (8 mg mL^{-1})	3D	Fluid flow effects on tumor-blood endothelial signaling and formation
Silvestri et al., 2020	HUVECs and primary human breast tumor specimens	PDMS coated with rat tail type I collagen (7 mg mL^{-1})	3D	Cancer cell effects on blood vessel permeability
Amann et al., 2017	HUVECs, primary human microvascular cells of lungs, A549, Colo699, SV-80	GravityPLUS microtissue culture system	3D	Cancer-mediated angiogenesis
Ko et al., 2019	HUVECS, normal human lung fibroblasts (NHLF), U87MG, HepG2	3D printed Sphero-IMPACT substrate with a polystyrene mold coated with fibrinogen (2.5 mg mL^{-1})	3D	Cancer-mediated angiogenesis
Cui et al., 2018	Mouse yolk sac derived endothelial cells	PDMS with $\alpha_v\beta_3$ integrin specific type I collagen hydrogel	3D	Cancer-mediated angiogenesis
Han et al., 2020	HUVECs, U87 MG, and NHLF	Gelatin and alginate solution (20% w/v) coated with fibrinogen solution (4% w/v)	3D	Drug testing
Hachey et al., 2021	Human endothelial colony-forming cell-derived endothelial cells, NHLF, and SW480	PDMS coated with fibrinogen (5 mg mL^{-1})	3D	Drug testing
Haase et al., 2020	HUVEC, NHLF, Skov3, and A549	PDMS with fibrin gel (3 mg mL^{-1})	3D	Drug transport through endothelial cells
Kwak et al., 2020	HUVECs, NHLF, and MDA-MB-231	PDMS with various concentrations of Matrigel, rat tail type I collagen and fibrinogen	3D	Extracellular matrix material effects on vessel stability and formation in vitro
Chen et al., 2013	HUVECs, NHLF, MDA-MB-231, HT-1080, and MCF-10A	PDMS injected with bovine fibrinogen and cell solution (5 mg mL^{-1})	3D	Tumor cell extravasation
Hajal et al., 2021	HUVECs, NHLF, MDA-MB-231	PDMS injected with a fibrinogen hydrogel	3D	Tumor cell extravasation and invasion
Azadi et al., 2021	HUVECs, MDA-MD-231, and MCF7	PDMS coated with various concentrations of collagen	3D	Substrate stiffness effects on tumor extravasation
Hikimoto et al., 2016	HUVECs, human dermal LECs, and HT29	Cell layering with fibronectin-gelatin nanofilms (10 nm thick)	3D	Metastasis and drug testing

vessel co-option or remodeling of neighboring blood vessels, overcome the inhibition.

Buchanan et al. developed a 3D microfluidic tumor vasculature model to observe the effects of flow and dimensionality on expression profiles.[61] Their model was created inside a fluorinated ethylene propylene (FEP) tube seeded with cancer cells that were embedded in a collagen hydrogel. A needle-punched microchannel was created, and BECs were seeded onto the walls of the microchannel. They compared their 3D model with 2D cultures with and without flow, and with mono- or cocultures. They found that MDA-MB-231 breast cancer cells expressed significantly higher levels of MMP-9, a collagenase, in 3D static culture compared to 2D. They also found that 3D culture with flow increased angiogenic genes PDGF-BB and angiopoietin 2 (ANGPT2), compared to 2D and static models. They concluded that their 3D model was a better representative model of the tumor microenvironment compared to 2D systems, emphasizing the advantages of a more complex model.

Tumor cells have substantial mechanical effects on vasculature. Inside the tumor, vessels have been observed to be mechanically compressed and collapsed. Blood vessel collapse was thought to be caused by the elevated interstitial fluid pressure; however, the microvascular pressure is equally large. Silvestri et al. developed a microfluidic blood vessel model by seeding human umbilical vein endothelial cells (HUVECs) in a 3D lumen as a platform to study cancer cell-induced vessel permeability.[62] Permeability was measured by perfusing the vessel with fluorescent dextran and comparing luminal and extra-luminal intensity. Introducing breast tumor organoids into the ECM induced an increase in vessel permeability across three dextran sizes: 3, 10, and 70 kDa. They quantified the number of focal defects and found a strong association between defect number and permeability ($r^2 = 0.75$). This indicated tumor-induced endothelial barrier dysfunction was driven by apoptosis of BECs. In the model, tumor cells were observed to invade the endothelium itself, forming a mosaic vessel. This phenomenon also occurs in cancer patients in vivo. Mosaic vessels allow cancer cells direct access into the vasculature, promoting metastasis and formation of precancerous niches. Using their model, the group tracked a mosaic vessel over a 24 h period and observed that cancer cell clusters break off from mosaic vessels and roll onto the luminal side in the direction of flow. Thus, their model was able to recapitulate the process of vessel permeability and cancer cell metastasis in vitro.

Amann et al. created a 3D hanging-drop cell culture method that includes cancer cells, fibroblasts, and endothelial cells to better recapitulate in vivo physiology.[63] They found that endothelial cell migration depends on proangiogenic factors including VEGF-A and bFGF. They also found that fibroblasts play a significant role in regulating cytokine and growth factor production essential for angiogenesis. These stimulators created a gradient, with high concentrations at the rim of the model and decreasing concentrations towards the core of the microtissue, the path which endothelial cells also take. The inclusion of fibroblasts in this model provided a more physiologically accurate representation of the environment that cancer cells reside, increasing the relevance of their findings.

Ko et al. developed a 3D tumor-angiogenesis microfluidic model that can be used for preclinical drug screening.[64] The group created sphero-IMPACT polystyrene injection mold that held glioblastoma spheroids surrounded by HUVECs in a liquid interface meniscus. The group stimulated this culture with either TNF-α or transforming growth factor β1 (TGF-β1) and measured cell migration and angiogenesis. The TGF-β1-stimulated cancer cells had the greatest migration distance, and the TNF-α stimulated cancer cells had the greatest migration area. In an angiogenesis assay, they tested three drugs on the cells and were able to determine the best drug candidate for blocking cancer-cell induced angiogenesis. This platform was made for large scale and reproducible drug testing purposes for cancer treatments, and their inclusion of angiogenesis and tumor migration assays provides the flexibility for testing of many drugs.

Cui et al. focused on the important role macrophages play in angiogenesis within the tumor microenvironment.[65] The group developed a 3D microfluidic model that consisted of a blood vessel and a glioblastoma tumor with tumor-treated macrophages. They found that glioblastoma-induced M2-like macrophages exhibit an anti-inflammatory property which led to EC proliferation and angiogenic sprouting. Conversely, classically activated M1-like macrophages suppressed angiogenic activity. They found there is perivascular macrophage-EC communication through integrin ($\alpha_v\beta_3$) receptors and Src-PI3K-YAP signaling. This model can be helpful in screening therapeutics for glioblastoma and is also a key way to better understand the immune components involved in tumor-mediated angiogenesis.

Han et al. developed a multicellular tumor spheroid in a microvascular network and studied chemotherapeutic efficacy.[66] Glioblastoma spheroids were cultured in a bioprinted hydrogel, and HUVEC and lung fibroblasts were integrated into the system using bioprinting. An anticancer drug, Temozolomide, and SU, a blood vessel inhibitor, synergistically decreased tumor size. This drug response is in accordance with mouse model and in vivo studies, thus validating the relevance of their in vitro model.

Hachey et al. verified the utility of their 3D vascularized microtumor (VMT) model of colorectal cancer (CRC) by comparing gene expression to in vivo studies and a 2D monolayer model.[67] An EC-lined lumen was cocultured with SW480, a CTC cell type, and human lung fibroblasts (HLF) in the stroma and luminal flow was introduced. The group observed upregulation of TGF-β signaling in HLF in the stroma of their 3D model, but not in 2D monoculture of spheroids. Enhanced stromal TGF-β signaling in tumor microenvironments is strongly associated with a poor CRC prognosis. Treating the model with TGF-βR1 antagonist, galunisertib, blocked SW480 growth in their 3D model, but not in tumor spheroid or monoculture. Their VMT highlighted the importance of tumor-associated fibroblasts in the development of tumors and as crucial components of in vitro models for therapeutic testing.

Haase et al. created a tumor spheroid-microvasculature model that included both luminal and stromal chemotherapeutic drug delivery via a microvessel.[68] First, the group observed increased vessel permeability in the presence of ovarian carcinoma (Skov3) and lung adenocarcinoma (A549) cells, suggesting increased transluminal transport. Skov3 induced local apoptosis events in the endothelium while A549

induced a broader distribution of apoptosis. Furthermore, they studied how Taxol, a common chemotherapy, modulates BEC barrier function. Without tumor spheroids, Taxol increased permeability 1 h after treatment in a dose-dependent manner due to drug-induced BEC apoptosis. They also found that tumor spheroids cultured alone shrank following Taxol treatment, but grew in size in the presence of microvasculature, indicating poor delivery of the chemical agent to the tumor cells. The group observed fibroblasts localization near the spheroids and depositing collagen III, an ECM protein, likely reduced diffusion of Taxol into the tumor. The group also measured a significant decrease in dextran diffusivity in the tumor spheroid and nearby stroma. This model demonstrated that the EPR effect for drug delivery may be limited by stromal cell and ECM barriers in the interstitial space and suggests that microfluidic platforms studying drug delivery must include stromal cells.

Kwak et al. developed a 3D microfluidic device combining luminal and interstitial flow to study blood vessel sprouting toward a tumor.[69] MDA-MB-231 breast cancer cells induced increased vessel sprouting in a fibrin-based Matrigel. Coculture with human lung fibroblasts was required for increased vessel sprouting by breast cancer cells. However, coculture with mesenchymal stem cells had no significant increase in vessel sprouting. This finding indicates that stromal fibroblasts are needed to recapitulate the tumor microenvironment and may contribute to cell signaling.

Wagenblast et al. identified vascular mimicry as a key pathway for breast cancer metastasis.[70] This process is separate to angiogenesis and resembles vasculogenesis observed in fetal development. They found that Serpin Family E Member 2 (SERPINE2) and secretory leukocyte peptidase inhibitor (SLPI) proteins were required for the tumor to develop its own vasculature. These proteins exhibited anti-coagulant properties to allow for vessel perfusion, indicating their use for cancer cell migration.

Extravasation is a key concept that needs to be understood when studying how cancer moves and spreads. Chen et al. modeled tumor cell extravasation in a 3D microfluidic platform across different cell types with increasing metastatic potential.[71] Their model consisted of a HUVEC-lined lumen connecting two media compartments in a coculture with nonhuman lung fibroblasts in a 3D ECM. First, the group verified their mature blood vessel model by observing physiologically relevant permeability, VE-cadherin staining, and collagen IV deposition in the blood vessel compartment. The group introduced MDA-MB-231 breast cancer cells into the lumen via flow and tracked cancer cell extravasation into the ECM via transendothelial migration (TEM). The vessel model was stimulated with pro-inflammatory cytokines typically upregulated in cancer patients, including interleukin-1β (IL-1β), TNF-α, and interleukin-6 (IL-6). These cytokines increased vessel permeability of dextran and TEM by 2.1 and 2.3-fold, respectively. Furthermore, the more metastatic cell type HT-1080 fibrosarcoma had a extravasation rate of 27.34 ± 4.9%, which was significantly greater than the less invasive MDA-MB-231 cell type which had a rate of 13.23 ± 3.2%. This model was one of the first to associate metastatic potential with extravasation rate out of the blood vessel. Future studies can use this model for preclinical testing of drugs that target cancer cell TEM.

Hajal et al. created 3D in vitro microvascular networks using HUVECs with hydrostatic pressures applied along and across endothelial layers to recapitulate both luminal and transendothelial flow.[72] They found that luminal flow promoted extravasation of tumor cells and that transendothelial flow increased the rate in which tumor cells migrated across the endothelium and in the matrix.

Azadi et al. was interested in seeing the effects of substrate stiffness on the extravasation of breast cancer cells using a microfluidic device. Their device consisted of a channel filled with collagen of different stiffnesses and breast cancer cells were seeded onto the matrix. Another channel was present specifically for seeding endothelial cells.[73] They found that a softer substrate caused a 46% reduction in breast cancer cell migration and decreased the migration distance up to 53%.

Another 3D model was created to test metastasis and drug testing. Hikimoto et al. demonstrated perfusable networks of BECs and LECs using a cell-layering technique consisting of fibroblasts, LECs or BECs, and 10 nm fibronectin gelatin films (Figure 3e).[57] This cell-layering technique induced spontaneous formation of vessels within the matrix of cells. Their model was able to mimic dextran diffusion into and out of the vessels, successfully recapitulating vessel function in vitro. They used their model for pharmacokinetic studies by seeding cancer cells within the blood vessel network and found increased cell death with the addition of anticancer treatment through the blood vessel network, which mimics intravascular drug administration in vivo. Overall, their model demonstrated an in vitro technique of vessel formation that could be used to more accurately test drug performance.

There are many more examples of models and we direct readers to reviews describing tumor angiogenesis[74] and the tumor-blood vessel microenvironment[75] for a full picture. In this brief overview, the field has created a better understanding of the EPR effect, tumor-induced angiogenesis, the importance of using relevant stromal cells, including fibroblasts, tumor cell extravasation and migration, the role of macrophages in tumor-induced angiogenesis, and the ability to use these platforms for high-throughput preclinical drug testing. This knowledge can be used to create more targeted drugs toward specific mechanisms in the cancer cells or endothelial cells to limit these processes that occur in cancer.

3.2. Tumor-Lymphatic Vessel Interactions

The cancer microenvironment is comprised of uncontrolled proliferation of cells, complex cell-matrix interactions, and upregulated cell signaling. Lymphatic vessels have increasingly become known for mediating metastasis of tumors.[76,77] The use of lymphatic vessels in modeling of the tumor microenvironment began within the last two decades and has progressed to provide more accurate models of the cancer microenvironment, along with elucidating interactions between cancer cells and lymphatic vessels (**Table 4**).

The earliest report of a cancer-lymphatic model was provided by Shields et al. in 2007 who studied the migration of tumor cells into lymphatic vessels (Figure 2c).[28] Using a Transwell model with a 2D LEC monolayer, they observed that the high

Table 4. Summary of tumor-lymphatic vessel in vitro models.

Author, year	Cell type	Model material	Dimension	Physiological process modeled
Shields et al., 2007	Human neonatal foreskin dermal LECs, MCF10A, MCF7, ZR75-1, MDA-MB-435S	Porous cell culture inserts with collagen (unknown concentration)	2D	Tumor cell migration to lymphatic endothelial cells
Frenkel et al., 2021	Immortalized human neonatal dermal LECs, HEK-293T	Organoplate coated in rat tail type I collagen (4 mg mL^{-1})	2D	Cancer-mediated lymphangiogenesis
Cho et al., 2021	Human dermal LECs, MDA-MD-231, BT474, and A549	PDMS coated with collagen type I (2 mg mL^{-1})	3D	Cancer-mediated lymphangiogenesis
Chung et al.,	HUVECs and human dermal LECs, NHLF, SK-OV3 and MKN-74	PDMS coated with fibrin (2.5 mg mL^{-1})	3D	Cancer mediated angiogenesis and lymphangiogenesis
Gong et al., 2019	Lymph node derived human LECs, HUVECs, and cancer associated fibroblasts	PDMS coated with fibronectin (33 µg mL^{-1})	3D	Effects of cancer on lymphatic vessel barrier integrity
Fathi et al., 2020	Primary human LECs	PDMS coated with fibronectin (2 µg cm^2)	3D	Effects of cancer-relevant cyclic flow and inflammatory cytokines on cell alignment and viability
Lugo-Cintron et al., 2020	Human LECs and MDA-MB-231	PDMS coated with rat tail type I collagen (3 mg mL^{-1} and 6 mg mL^{-1})	3D	Effects of ECM density and cancer cells on lymphatic vessel barrier integrity
Cao et al., 2019	HUVECs, human LECS, and MCF-7	PDMS coated with gelatin methacryloyl (GelMA) matrix	3D	Drug testing
Harris et al., 2018	Human dermal LECs, human mammary fibroblasts, HCC 38 and HCC 1806	Transwell coated with rat tail type I collagen (0.18 mg mL^{-1})	2D	Drug testing
Harris et al., 2018	Human dermal LECs, HCC38, HCC1806, and MDA-MD-231	Transwell coated with rat tail type I collagen (0.18 mg mL^{-1})	2D	Drug testing
Nishiguchi et al., 2018	Human dermal fibroblasts, HUVECs, hLECs, MiaPaCa-2, BxPC3, and HT29	Transwell with cell layers of fibroblasts and 26 nm fibronectin-gelatin nanofilms	3D	Cancer metastasis
Pisano et al., 2015	Human dermal neonatal foreskin LECs and MDA-MB-231	Transwell coated with collagen (unknown concentration)	2D	Transendothelial cancer cell migration
Ayuso et al., 2020	Lymph node derived LECs, MCF7, and MDA-MB-231	PDMS coated with rat tail type I collagen (3 mg mL^{-1})	3D	Cancer cell conditioning of lymphatic vessels

expression of CC-chemokine ligand 7 (CCR7) on cancer cells created an invasive response that was attracted to the CCL21 gradient provided by LECs. The amount of migration depended on the cancer cell type and CCR7 and CCL21 concentrations. Additionally, they found that the pleckstrin homology domain of protein kinase B(AKT) (PHAKT) was relocated to the plasma membrane, indicating cell movement, and Rac1 localization at the leading edge of the cell, indicating migratory polarization.

More recent studies have determined the effects of cancer cells on lymphangiogenesis. Frenkel et al. created an immortalized cell line of LECs and modeled lymphangiogenesis and cancer responses using an Organoplate consisting of three 3D tubes coated in collagen.[78] Their cells responded to VEGF, bFGF, S1P, and PMA stimulation with lymphatic sprouting. Additionally, they were able to show cancer cell-induced lymphatic sprouting. They concluded that their cell line was valid and could model lymphangiogenesis and cancer cell interactions for up to 14 days. Additionally, the use of the immortalized cells can increase throughput and provide reproducibility that is difficult to achieve with primary cells.

Cho et al. used a PDMS collagen hydrogel 3D model to show sprouting of lymphatic vessels towards a tumor, and increased signals of CCL21 in LECs and CCR7 in the cancer cells.[79] Stimulation with VEGF-C gradient induced sprouting. Interstitial flow with VEGF-A and VEGF-C induced lymphangiogenesis and aligned cells parallel to flow direction. They concluded that this in vitro model provides a good platform to study the relationship between cancer and lymphatic vessels. Additionally, Chung et al. used a 3D microfluidic channel with one central channel surrounded with either fibroblasts or cancer cells to study angiogenic and lymphangiogenic interactions[56] (Figure 3b). They found that there was both angiogenic and lymphangiogenic sprouting toward the tumor-fibroblast coculture. Thus, their model was able to show simultaneous sprouting in response to cancer cells, and platforms such as this can be used for drug discovery or personalized medicine in the future.

Additionally, permeability effects of cancer cells have been studied in many microfluidic models. Gong et al. created a 3D in vitro model of a lymphatic vessel using PDMS and a needle-punched lumen.[80] They characterized the vessel as compared to a blood vessel and found that under interstitial flow, LECs aligned parallel to the flow direction and the permeability of 10 kDa and 70 kDa dextran was higher in the lymphatic vessel than in the blood vessel. Stimulation with VEGF-C increased IL-8, endothelin-1, and follistatin concentrations. When cocultured with cancer-associated fibroblasts, levels of both protumorigenic growth factors, granulocyte colony stimulating factors (G-CSF) and HGF, and proinflammatory cytokines, IL-6 and IL-8 increased in the model. Both prolymphangiogenic and protumorigenic stimulation increased vessel permeability,

indicating vessel leakage which can promote cancer cell migration.

Another 3D microfluidic model developed by Fathi et al. studied the effect of cancer relevant interstitial flow on LECs using gravity-driven flow via an Arduino microcontroller.[81] They varied the flow speed to induce shear stress levels of a highly metastatic tumor niche (no flow), a healthy lymphatic vessel (low flow), and lymphatic vessels near a tumor site (high flow). Their results showed that flow reduces LEC TNF-α and IL-8 production, which are correlated with junction barrier regulation. In the presence of interstitial flow, they found that LECs created more stable structures, as indicated by high cell viability, and aligned parallel to the direction of flow. This study showed the importance of using interstitial flow conditions that are relevant to the type of system the model is replicating.

Lugo-Cintron et al. created a 3D microfluidic device with a lymphatic vessel that tested the effects of collagen density on lymphatic vessel permeability and cancer-lymphatic interactions.[82] They found that the permeability of LECs increases with high density collagen (6 mg mL^{-1}), and the barrier function is regulated by IL-6. Higher collagen densities upregulate the pro-inflammatory cytokines TNF-α, IL-1α, CCL19, CCL21, C-X3-C motif chemokine ligand 1 (CX3CL1), IL-1β, IL-6, IL-8, and C-X-C motif chemokine ligand 12 (CXCL12) in LECs. When cancer cells were added, the permeability decreased in both low (3 mg mL^{-1}) and high-density models (6 mg mL^{-1}). This decrease was also dependent on IL-6. They concluded that the effects of IL-6 on lymphatic permeability can be a potential target for therapeutics to inhibit metastasis through the lymphatic vasculature.

Several models have also studied the effects of lymphatics on cancer therapeutic delivery and efficacy. Cao et al. created a 3D microfluidic model containing blood and lymphatic vessels surrounded by a tumor chamber consisting of MCF-7 cells in a gelatin methacryloyl matrix.[83] They tested the diffusion of Fluorescein isothiocyanate (FITC)-dextran and an anticancer drug, doxorubicin, from the center of the tumor chamber to their two-channel system without BECs or LECs present in the channels. They found that the presence of both the blood and lymphatic vessels increased the diffusion rate of both molecules compared to the presence of a blood vessel only. This resulted in a less effective treatment of the cancer cells, as indicated by a 20% higher cell viability, due to the additional drainage of the drug from the lymphatic vessel. They concluded that this system consisting of blood and lymphatic vessels was a highly relevant model of a tumor environment in vivo. In the future it can be used as a drug screening platform to determine accurate dosing for anticancer drugs. Harris et al. created a Transwell model to study the effects of the drug doxorubicin.[84] They simulated a lymphatic vessel using a 2D LEC monolayer on the bottom layer of the Transwell, and they simulated tumor on the top layer using fibroblasts and breast cancer cells embedded in a collagen matrix. When testing the efficacy of the anticancer treatment, they found that there was a dose-dependent increase of cell death, with 70% cell death in the HCC38 cell line and 35% cell death in the HCC1806 line. This correlated with the amount of invasion through the LEC monolayer between each cell line, where HCC38 cells invaded less compared to HCC1806. Therefore, their Transwell model was useful in detecting changes in chemotherapy efficacy between different cell lines in terms of cell death and invasion through a lymphatic monolayer.

The same 2D model was used again by Harris et al.[85] to look at the efficacy of docetaxel on cancer cell invasion through lymphatics. Using breast cancer cell lines HCC38, HCC1806, and MDA-MB-231, they found that the addition of docetaxel increased cancer cell invasion through the LEC monolayer for the HCC38 and MDA-MB-231 cell lines. The HCC1806 cell line response was negligible. Using the same model, they added an anti-VEGFR3 treatment to reduce the invasive response of cells to docetaxel. They found that the anti-VEGFR3 treatment, MAZ51, in addition to docetaxel, was able to reduce the invasive response more than docetaxel alone. This response was only seen in the HCC38 and MDA-MB-231 cells. They concluded that their model was able to show that combining docetaxel with MAZ51 could reduce the harmful effects of docetaxel, which includes increased invasiveness into lymphatics. The harmful effects of docetaxel were also seen in vivo using a breast cancer 4TI mouse model, where docetaxel increased lymphangiogenic markers VEGF-C and TNF-α. These effects were mitigated with the addition of anti-VEGFR3 treatment. These results further validated the use of the in vitro model for predicting drug effects in vivo.

A number of models have also studied cancer cell invasion and migration. Nishiguchi et al. created a 3D cancer cell model with LECs and BECs using a cell layering technique with stromal fibroblasts and nanofilms.[86] They modeled cancer cell invasion into lymphatic capillaries with the pancreatic cancer cell line BxPC3. They showed that this interaction was due to an increase in MMP-7 and MMP-9. They concluded that their model could be useful for the preclinical assessment of intravasation-targeted drugs. Pisano et al. used a Transwell model with LECs and MDA-MB-321 cancer cells to study the interactions due to luminal and transmural flow.[87] They observed a luminal flow-dependent increase for cancer cells to transmigrate across the lymphatic endothelium due to CCL21 upregulation in LECs and CCR7 signaling in cancer cells. Addition of transmural flow increased this transmigration rate, but further study is needed to understand the mechanism behind this effect.

Ayuso et al. studied the interactions between a lymphatic vessel and cancer cells with a two-vessel 3D microfluidic chip.[88] They tested interactions between LECs and breast cancer cell lines MCF-7 (estrogen receptor-positive) and MDA-MB-231 (triple negative). They found LECs interacting with MCF-7 cells had upregulated pro-lymphangiogenic genes including VEGF-C, indicating these cancer cells can induce lymphangiogenesis. This effect was not seen in the triple negative MDA-MB-231 cell line. However, when analyzed for lymphangiogenic sprouting, they found sprouts from lymphatic cells culture with both cell lines. MCF-7 cells also increased the expression of epithelial-mesenchymal-associated genes in the lymphatic cells, along with increased proliferative and reduced apoptotic genes in the lymphatic cells. The MDA-MB-231 cell line had a negligible effect on the production of these genes in lymphatic cells. When testing the permeability of lymphatic vessels, they found that there was an overall increase in permeability for both cell lines in the coculture model compared to monocultures. There was a higher increase for LECs cultured with MCF-7 cells compared to MDA-MB-231 cells (2.6-fold vs 1.8-fold for glucose, and

Table 5. Summary of inflammatory blood vessel and immune cell in vitro models.

Author, year	Cell type	Model material/type	Dimension	Physiological process, modeled
Mondadori et al., 2021	HUVECs, human primary monocytes isolated from buffy coats	PDMS coated with fibrin and human fibronectin (10 μg mL^{-1})	3D	Monocyte extravasation in osteoarthritis
Perez-Rodriguez et al., 2021	HUVECs and THP-1 monocytes	PDMS coated with rat tail type I collagen (2.5 mg mL^{-1} and 6 mg mL^{-1})	3D	Monocyte extravasation from blood vessels
Nam et al., 2020	HUVECs and THP-1 monocytes	PDMS coated with rat tail type I collagen (2 mg mL^{-1})	3D	Monocyte adhesion in inflammatory conditions
Venugopal Menon et al., 2018	HUVECs, THP-1 monocytes, and whole blood	PDMS	3D	Leukocyte activity in atherosclerosis
Lee et al., 2014	HUVECs and THP-1 monocytes	Transwell	2D	Anti-inflammatory effects of flavonoids
Cellesen et al., 2021	Human arterial endothelial cells, human saphenous vein endothelial cells, human microvascular lung endothelial cells	Transwell coated with 0.5% gelatin	2D	Permeability of blood vessels in anaphylaxis

6.1-fold vs 4.4-fold for dextran, respectively). Overall, they found that the specific cancer cell types modulated LECs differently, and these differences can be determined using this in vitro model to determine better therapeutic options.

Overall, these models have been developed to understand the complex interactions between tumors and lymphatic vessels. The interactions studied in these models, including cancer cell migration, vessel permeability, and effects of interstitial flow were able to be decoupled from complex in vivo physiology to make conclusions about how cancer cells affect lymphatic vessels. Further progress of these models can lead to discovery of drug targets and improve design of personalized medicines for cancer treatment.

3.3. Vascular Inflammation and Immune Cell Extravasation

There are multiple conditions that can affect the vascular system which include both autoimmune and inflammatory diseases. While this review will focus on vascular inflammation and its effect on immune cells (**Table 5**), readers are directed to a review by Schwartz et al.[89] to learn more about the effects of autoimmune disease on lymphatic function. During inflammation, the structure of blood vessels changes to support the migration of a variety of immune cells. The transport of immune cells through the blood vessel to the targeted area and out to the tissue is a key aspect in vascular function (**Figure 4**a).

Two groups looked specifically at monocyte extravasation and how it affects different physiological conditions. Mondadori et al. aimed to characterize the accumulation of extravasation of monocytes due to macrophages in the synovium of osteoarthritis (OA) patients.[90] They created a 3D device with a channel for synovial fluid, two channels for the synovial matrix, a channel for endothelial cells, and a channel for the cartilage matrix. They found that the number of extravasated monocytes out of the endothelial compartment increased in response to patient OA synovial fluid and to a mix of chemokines (CCL2, 3, 4, and 5). In addition, they found that blocking both CCR2 and CCR5 was more effective in blocking monocyte extravasation compared to blocking CCR2 alone. Another group looked at the effects of flow on monocyte extravasation. Pérez-Rodríguez et al. created a microfluidic model with a needle-punched lumen that held endothelial cells embedded within a collagen matrix.[91] They found that vessels perfused with flow had more monocytes adhered to the vessel wall, but less monocytes extravasated out of the vessel. This suggests that there is reduced vessel permeability and increased vessel integrity in the presence of flow.

Proper blood vessel response during inflammation is essential to ensure that the inflammatory response is neither excessive nor nonresolving, which could cause diseases such as atherosclerosis, sepsis, and vasculitis.[92] Lipopolysaccharides (LPS), components of gram-negative bacteria, cause an inflammatory response in the body which could lead to liver damage, neurological degradation, and initiate an inflammatory response to the endothelial lining of blood vessels. Nam et al. used a 3D microfluidic device to look at the effects of LPS delivered to the basal side of the blood vessel to mimic the presence of bacteria in the body.[92] They first looked at expression of intercellular adhesion molecule 1 (ICAM-1) in BECs, a key molecule involved in leukocyte adhesion and transendothelial migration that is normally upregulated by inflammatory stimuli. Compared to unstimulated conditions, ICAM-1 increased over time at 4 h (22.04 ± 4.05%), 8 h (36.25 ± 5.51%) and 12 h (61.81 ± 6.81%), all compared to 0 h (9.31 ± 1.37%). They also looked at VE-cadherin which is normally downregulated during inflammation. In their model they found that VE-cadherin expression was lower at 4 h and 8 h compared to baseline. Lastly, they looked at monocyte adhesion and migration in the presence of LPS.[93] The group calculated the number of affected cells by taking the sum of the number of adhered cells to endothelium and number of cells that have undergone transendothelial migration into collagen. They found that there were significantly higher (1103.5 ± 95.4) affected cells in normal conditions and the number of affected cells increased 4 h (1360.5 ± 98.5) and 8 h (1737.6 ± 183.3) after LPS treatment. The number of cells that underwent transendothelial migration increased from control (20 ± 3.4) to 4 h (26 ± 6.5) and 8 h (34.8 ± 6.4) after LPS treatment. Overall, this model showed that immune cell migration tended to increase with longer LPS stimulation.

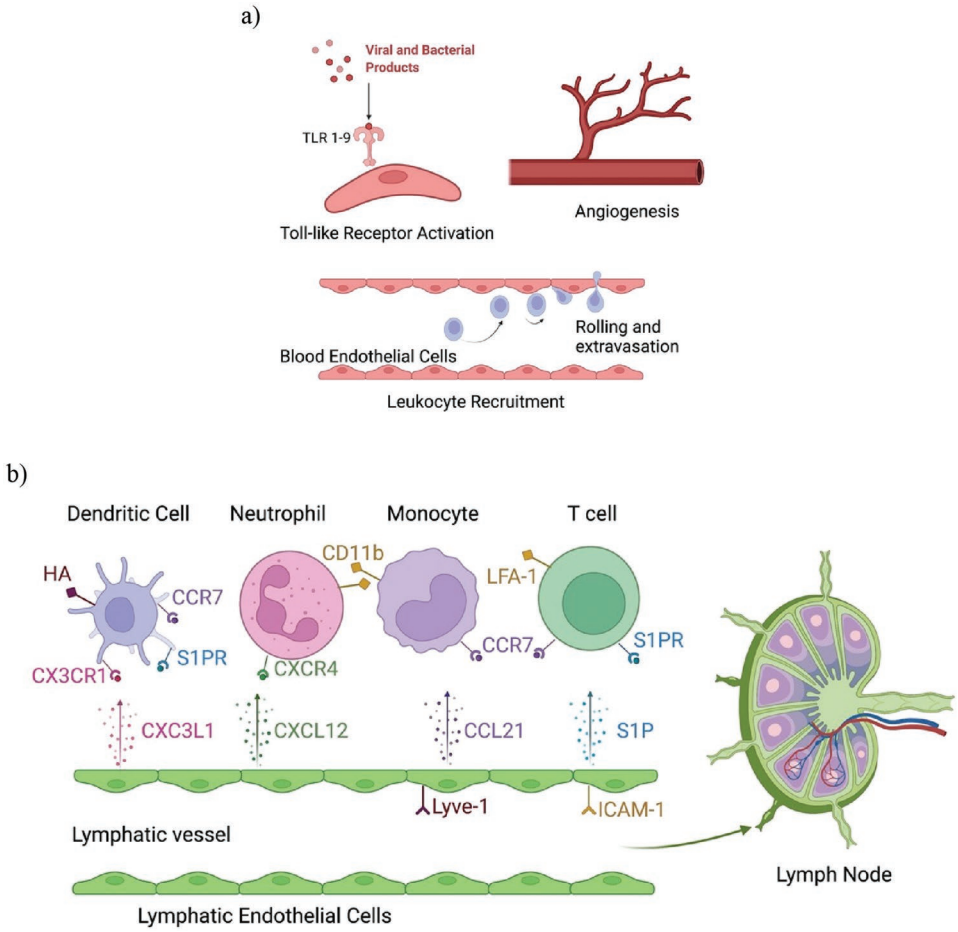

Figure 4. Schematic illustrating the interactions between immune cells and blood and lymphatic endothelium. a) Endothelial cells play roles in various aspects of the immune system including expression of toll like receptors (TLRs), angiogenesis induced by factors secreted by immune cells during inflammation, and leukocyte recruitment in adaptive immunity. b) Lymphatic vessels play a large role in immune cell migration to lymph nodes, and produce a number of chemokines such as CCL21, CX3CL1, S1P, and CXCL12 and adhesion molecules such as Lyve-1 and ICAM-1 that help regulate transendothelial migration. Created with BioRender.com.

Atherosclerosis is the leading cause of cardiovascular disease and is caused by an accumulation of cholesterol-containing, low-density lipoproteins in the sub-endothelial space.[94] It is caused by the interaction between inflamed endothelial cells and activated monocytes, macrophages, and T cells. Atherosclerosis typically affects areas based on its architecture and preferentially affects bifurcations in vessels, as these regions lack shear stress.[15] Many 2D and 3D models have attempted to model atherosclerosis, but these models do not include vascular geometries, BECs, blood components, and complex flow profiles found in vivo. Menon et al. developed a 3D stenosis blood vessel model that incorporates hemodynamics and the interplay between leukocytes and endothelial cells.[94] The group first looked at the adherence of the monocyte cell line THP-1 on a monolayer of HUVECs in a microfluidic device. They found that when the monocytes were perfused at 1 dyne cm^{-2}, cells adhered to both 50%- and 80%-constricted channels. The channels were constricted by changing the width of the channel that cells were able to adhere to. However, when perfusion was increased to 10 dyne cm^{-2}, adherence only occurred in 80%-constricted channel. Next, the group looked at vascular inflammation during flow by perfusing media containing TNF-α over the HUVEC at 1 dyne cm^{-2}. They found that HUVECs only aligned with the direction of flow on the lateral sides of the stenosis (areas of higher shear). ICAM-1 expression was 4 times higher in the HUVECs in the TNF-α perfused device compared to controls, and was found to have similar levels in the 50%- and 80%-constricted channels in the presence of TNF-α. However, in the 80%-constricted channel, ICAM-1 levels were higher in stenosis compared to nonstenosis regions. The group then wanted to investigate leukocyte-endothelial interactions in the presence of whole blood. They perfused healthy whole blood into both healthy and TNF-α treated HUVECs in the device at 1 dyne cm^{-2}. They saw a linear trajectory in the 50%-constricted channel and a lower velocity and curvilinear trajectory in the 80%-constricted channel. They found that in the healthy model, only the 80%- constricted channel had significant leukocyte adherence. Finally, they investigated the levels of neutrophil and monocyte adhesion in the inflamed model. It was found that there were twice as many neutrophils than monocytes that adhered in the 50%-constricted channel, while

Table 6. Summary of lymphatic vessel and immune cell in vitro models.

Author, Year	Cell type	Model material/type	Dimension	Physiological process, modeled
Xiong et al., 2017	Primary mouse and human LECs, Ms-1 cells, SVEC-10, MCF-7, MDA-MB-231	Transwell coated with 0.2% wt/vol gelatin	2D	T cell and Leukocyte trans-lymphatic endothelial migration
Miteva et al., 2010	Human neonatal foreskin derived LECs and dendritic cells	Transwell coated with rat tail Type I collagen (50 μg mL^{-1})	2D	Dendritic cell trans-lymphatic migration
Brown et al., 2018	Primary human dermal LECs	Transwells coated with bovine collagen (unknown concentration)	2D	Lymphatic guided dendritic cell migration

there was a 3-fold increase in monocyte adhesion in the stenosis portion only of the 80%-constricted channel. This model can pave the way for future work in investigating the interaction between inflammation and endothelium. Models such as this can be used to screen potential therapeutics and can be a way to profile blood for specific diseases.

In addition to studying the pathobiology of LPS-induced inflammation, several groups have used in vitro model systems to develop new therapeutic avenues. Lee et al. used baicalin, baicalein, and wogonin, variations of flavonoids found in plants, to help mitigate the inflammatory response against LPS.[95] They used a 2D monolayer of HUVECs to assess the permeability of the different compounds across the endothelium. When they delivered LPS and each of the compounds to HUVEC monolayers, they found that there was a decrease in transport of Evans blue-bound albumin across the monolayer with increasing concentrations of each drug (0×10^{-6}, 5×10^{-6}, and 10×10^{-6} M). This suggests that the compounds can maintain barrier integrity in a dose-dependent manner. Toll-like receptor 4 (TLR4) expression on HUVECs is a hallmark of inflammation and was seen to increase 4-fold when exposed to LPS. When HUVECs were stimulated with LPS, their TLR4 expression increased 4-fold. However, treatment with each drug significantly inhibited TLR4 expression. Many models including this one can help screen for therapeutics at a much faster rate than in vivo. While there is still work in getting in vitro models to be perfectly physiologically relevant, recent efforts showcase this possibility.

Cellesen et al. used a 2D Transwell model to study the effects of fast-acting mediators [histamine and platelet-activating factor (PAF)] and slow-acting mediators (thrombin) in anaphylactic conditions using three different BEC phenotypes: human arterial BECs (HAECs), human saphenous vein BECs (HSVECs), and human microvascular lung BECs (HMLECs).[96] There was no significant change in permeability of each BEC phenotype when stimulated with histamine, PAF, and thrombin. There was a slight decrease in permeability in HAECs in response to histamine and an increase in permeability in HMLECs in response to thrombin and a slight increase in permeability in response to PAF.

Overall, the design of these models allowed for the study of specific diseases such as OA and atherosclerosis, and were able to probe how factors such as shear force and histamine affect the inflammatory response of blood vessels. The insights into blood vessel physiology that these models provide have progressed the understanding of how these diseases affect immune and blood endothelial cells. Further progress in the development of these models can be useful for providing more knowledge of the relationship between immune-endothelial cells.

3.4. Modeling Immune Cell Migration via Lymphatics

Lymphatic vessels shuttle lymphocytes, antigen-presenting cells, and other immune cells from peripheral tissues to the lymph nodes, where the adaptive immune response is shaped (Figure 4b). Understanding the mechanisms underlying this migration is crucial both for developing new therapeutic interventions and understanding disease mechanisms. Several in vitro model systems study translymphatic migration of immune cells (**Table 6**). Xiong et al. created a 2D Transwell model with a monolayer of LECs on the underside of the PET membrane and demonstrated the migration of CD4 T cells across LECs from the basal to apical surfaces of the Transwell.[97] They found that this migration was due to CCL19 and CCL21 signaling and the receptors integrin $\alpha 4\beta 1$ (VLA-4) and VCAM-1. CD4 T cell migration increased under fluid flow through the Transwell and after stimulation with pro-inflammatory markers TNF-α and interferon-γ (IFNγ), which enhanced the expression of cell receptors and ligands in the culture. This model was able to show the specific mechanisms of migration and can be used to model other migratory mechanisms of other cell types in the future.

Miteva et al. demonstrated the migration of dendritic cells using transmural flow across a 2D monolayer of LECs on the top layer of the PET membrane.[98] The presence of flow delocalized VE-cadherin and PECAM-1 junctional proteins, and increased the expression of CCL21, ICAM-1, VCAM-1, and E-selectin. They found that transendothelial migration of dendritic cells was due to the increased CCL21 expression and CCR7 chemotaxis gradient, along with ICAM-1, VCAM-1, and E-selectin. They concluded that transmural flow overall increased transendothelial migration of dendritic cells.

LEC-derived exosomes induce DC migration into lymphatics by forming an exosome halo. Brown et al. performed proteomic analysis on these exosomes following TNF-α stimulation and identified that 86% of the 1700 proteins were upregulated, and most constituted a migratory protein signature. They observed a 1.6-fold increase in exosomes per mL in TNF-α stimulated primary human LECs and observed a 2.8-fold increase in exosome signaling halo in excised lymphatic vessels from patients with chronic kidney inflammation compared to healthy controls. CX3CR1 was required for enhanced DC migration and recognition of its ligand CX3CL1, found on LEC signaling exosomes.[99] These models have been successful in observing intercellular

interactions and can be used to further understand more complex relationships through future development (Tables 1–5).

4. Conclusions

In this review, we summarized the reported blood and lymphatic vessel in vitro models in 2D, 3D, with cancer interactions, and other inflammatory diseases. We also described immune communication through the vasculature and its importance for overall organ function. While 2D in vitro models are important in getting a better understanding of basic mechanisms, more complex 3D models are needed to better recapitulate physiological conditions. The presence of mechanical stimuli such as flow and cyclic pressure are important aspects of vessel functions. Many cell types interact during healthy and diseased states, and many 2D models do not include multiple cell types, generating models that lack important cell–cell communication. These challenges have been addressed in the developed 3D models, and we expect that future developments will be able to answer more questions regarding blood and lymphatic vascular physiology. These questions include how lymphangions regulate lymphatic flow in collecting vessels, and how transendothelial transport differs between initial and collecting lymphatic vessels. It is also important when designing these models to understand the effects of all the factors that are used in a model, including ECM, presence of flow, and presence of stromal cells. These factors should be incorporated when needed to ensure that the models are relevant to what is seen in vivo in the specific process being modeled. All of these efforts will lead the field to finding and testing more informed treatments in the clinic that can improve the lives of patients with diseases such as cancer or inflammation. While no system will ever be an exact replica of physiological systems, the strive to create more complex systems will help propel research in a more progressive path.

Acknowledgements

A.B. and A.R. contributed equally to this work. Funding for research was received from the University of Maryland Clark Doctoral Fellowship and National Institute of Health Maximizing Investigators' Research Award (MIRA) (R35). Michele Kaluzienski helped with copyediting and proofreading of this review.

Conflict of Interest

The authors declare no conflict of interest.

Keywords

blood vessels, endothelial-immune cell interactions, extracellular matrix, homeostasis, in vitro model, lymphatic vessels, microfluidics

Received: February 18, 2022
Revised: May 10, 2022
Published online: June 25, 2022

[1] R. N. Pittman, *The Circulatory System and Oxygen Transport*, Morgan & Claypool Life Sciences, San Rafael (CA): Morgan & Claypool Life Sciences; **2011**.
[2] M. Swartz, *Adv. Drug Delivery Rev.* **2001**, *50*, 3.
[3] N. L. Trevaskis, L. M. Kaminskas, *Nat. Rev. Drug Discov.* **2015**, *14*, 781.
[4] R. Shayan, M. G. Achen, S. A. Stacker, *Carcinogenesis* **2006**, *27*, 1729.
[5] H. R. Hampton, T. Chtanova, *Front. Immunol.* **2019**, *10*, 1168.
[6] V. Muzykantov, S. Muro, *Int. J. Transp. Phenom.* **2011**, *12*, 41.
[7] F. L. Miles, F. L. Pruitt, K. L. van Golen, C. R. Cooper, *Clin. Exp. Metastasis* **2008**, *25*, 305.
[8] Y. Shao, J. Saredy, W. Y. Yang, Y. Sun, Y. Lu, F. Saaoud, C. Drummer, C. Johnson, K. Xu, X. Jiang, H. Wang, X. Yang, *Arterioscler., Thromb., Vasc. Biol.* **2020**, *40*, e138.
[9] W. L. Olszewski, *Lymphatic Res. Biol.* **2003**, *1*, 11.
[10] W. Schmid-Schrauben, *Microlymphatics Lymph Flow* **1990**, *70*, 42.
[11] P. Baluk, J. Fuxe, H. Hashizume, T. Romano, E. Lashnits, S. Butz, D. Vestweber, M. Corada, C. Molendini, E. Dejana, D. M. McDonald, *J. Exp. Med.* **2007**, *204*, 2349.
[12] K. Alitalo, *Nat. Med.* **2011**, *17*, 1371.
[13] S. Fleischer, D. N. Tavakol, G. Vunjak-Novakovic, *Adv. Funct. Mater.* **2020**, *30*, 1910811.
[14] A. Aspelund, M. R. Robciuc, S. Karaman, T. Makinen, K. Alitalo, *Circ. Res.* **2016**, *118*, 515.
[15] K. H. K. Wong, J. M. Chan, R. D. Kamm, J. Tien, *Annu. Rev. Biomed. Eng.* **2012**, *14*, 205.
[16] Y. M. Shin, H. J. Shin, Y. Heo, I. Jun, Y.-W. Chung, K. Kim, Y. M. Lim, H. Jeon, H. Shin, *J. Mater. Chem. B* **2017**, *5*, 318.
[17] C. P. Ng, C.-L. E. Helm, M. A. Swartz, *Microvasc. Res.* **2004**, *68*, 258.
[18] C.-L. E. Helm, A. Zisch, M. A. Swartz, *Biotechnol. Bioeng.* **2007**, *96*, 167.
[19] C. Bonvin, J. Overney, A. C. Shieh, J. B. Dixon, M. A. A. M. Swartz, *Biotechnol. Bioeng.* **2010**, *105*, 982.
[20] K. L. S. Chan, A. H. Khankhel, R. L. Thompson, B. J. Coisman, K. H. K. Wong, J. G. Truslow, J. Tien, *J. Biomed. Mater. Res.* **2014**, *102*, 3186.
[21] A. R. Henderson, I. S. Ilan, E. Lee, *Microcirculation* **2021**, *28*, e12730.
[22] S. R. Moses, J. J. Adorno, A. F. Palmer, J. W. Song, *Am. J. Physiol.: Cell Physiol.* **2020**, *320*, C92.
[23] J. Keaney, M. Campbell, *FEBS J.* **2015**, *282*, 4067.
[24] M. W. Dewhirst, T. W. Secomb, *Nat. Rev. Cancer* **2017**, *17*, 738.
[25] Y. Li, K. Zhu, X. Liu, Y. S. Zhang, *Curr. Drug Metab.* **2018**, *19*, 100.
[26] V. Triacca, E. Güç, W. W. Kilarski, M. Pisano, M. A. Swartz, *Circ. Res.* **2017**, *120*, 1440.
[27] J. B. Dixon, S. Raghunathan, M. A. Swartz, *Biotechnol. Bioeng.* **2009**, *103*, 1224.
[28] J. D. Shields, M. E. Fleury, C. Yong, A. A. Tomei, G. J. Randolph, M. A. Swartz, *Cancer Cell* **2007**, *11*, 526.
[29] H. Wiig, M. A. Swartz, *Physiol. Rev.* **2012**, *92*, 1005.
[30] J. W. Breslin, K. M. Kurtz, *Lymphatic Res. Biol.* **2009**, *7*, 229.
[31] J. B. Dixon, *Ann. N. Y. Acad. Sci.* **2010**, *1207*, E52.
[32] P. Tso, J. A. Balint, *Am. J. Physiol.* **1986**, *250*, G715.
[33] J. S. Alexander, V. C. Ganta, P. A. Jordan, M. H. Witte, *Pathophysiology* **2010**, *17*, 315.
[34] A. L. Reed, S. A. Rowson, J. B. Dixon, *Pharm. Res.* **2013**, *30*, 3271.
[35] G. M. Price, K. M. Chrobak, J. Tien, *Microvasc. Res.* **2008**, *76*, 46.
[36] R. L. Thompson, E. A. Margolis, T. J. Ryan, B. J. Coisman, G. M. Price, K. H. K. Wong, J. Tien, *J. Biomed. Mater. Res.* **2018**, *106*, 106.
[37] M. Sato, N. Sasaki, M. Ato, S. Hirakawa, K. Sato, K. Sato, *PLoS One* **2015**, *10*, e0137301.
[38] R. H. Adams, K. Alitalo, *Nat. Rev. Mol. Cell Biol.* **2007**, *8*, 464.
[39] V. L. Bautch, K. M. Caron, *Cold Spring Harb. Perspect. Biol.* **2015**, *7*, a008268.
[40] K. Alitalo, T. Tammela, T. V. Petrova, *Nature* **2005**, *438*, 946.

[41] M. Shibuya, *Genes Cancer* **2011**, *2*, 1097.
[42] K. Alitalo, P. Carmeliet, *Cancer Cell* **2002**, *1*, 219.
[43] S. A. Stacker, S. P. Williams, T. Karnezis, R. Shayan, S. B. Fox, M. G. Achen, *Nat. Rev. Cancer* **2014**, *14*, 159.
[44] P. Carmeliet, *Nature* **2005**, *438*, 932.
[45] B. Vailhé, D. Vittet, J.-J. Feige, *Lab Invest.* **2001**, *81*, 439.
[46] K. T. Morin, R. T. Tranquillo, *Exp. Cell Res.* **2013**, *319*, 2409.
[47] S. L. Natividad-Diaz, S. Browne, A. K. Jha, Z. Ma, S. Hossainy, Y. K. Kurokawa, S. C. George, K. E. Healy, *Biomaterials* **2019**, *194*, 73.
[48] T. Davidov, Y. Efraim, N. Dahan, L. Baruch, M. Machluf, *FASEB J.* **2020**, *34*, 7745.
[49] S. Lee, M. Chung, S.-R. Lee, N. L. Jeon, *Biotechnol. Bioeng.* **2020**, *117*, 748.
[50] J. Pauty, R. Usuba, I. G. Cheng, L. Hespel, H. Takahashi, K. Kato, M. Kobayashi, H. Nakajima, E. Lee, F. Yger, F. Soncin, Y. T. Matsunaga, *EBioMedicine* **2018**, *27*, 225.
[51] F. Bruyère, L. Melen-Lamalle, S. Blacher, G. Roland, M. Thiry, L. Moons, F. Frankenne, P. Carmeliet, K. Alitalo, C. Libert, J. P. Sleeman, J.-M. Foidart, A. Noël, *Nat. Methods* **2008**, *5*, 431.
[52] T. Osaki, J. C. Serrano, R. D. Kamm, *Regen. Eng. Transl. Med.* **2018**, *4*, 120.
[53] L. Gibot, T. Galbraith, B. Kloos, S. Das, D. A. Lacroix, F. A. Auger, M. Skobe, *Biomaterials* **2016**, *78*, 129.
[54] S. Kim, M. Chung, N. L. Jeon, *Biomaterials* **2016**, *78*, 115.
[55] S. Landau, A. Newman, S. Edri, I. Michael, S. Ben-Shaul, Y. Shandalov, T. Ben-Arye, P. Kaur, M. H. Zheng, S. Levenberg, *Proc. Natl. Acad. Sci. USA* **2021**, *118*, e2101931118.
[56] M. Chung, J. Ahn, K. Son, S. Kim, N. L. Jeon, *Adv. Healthcare Mater.* **2017**, *6*, 1700196.
[57] D. Hikimoto, A. Nishiguchi, M. Matsusaki, M. Akashi, *Adv. Healthcare Mater.* **2016**, *5*, 1969.
[58] D. Kalyane, N. Raval, R. Maheshwari, V. Tambe, K. Kalia, R. K. Tekade, *Mater. Sci. Eng., C* **2019**, *98*, 1252.
[59] M. B. Schaaf, A. D. Garg, P. Agostinis, *Cell Death Dis.* **2018**, *9*, 115.
[60] Y. Tang, F. Soroush, J. B. Sheffield, B. Wang, B. Prabhakarpandian, M. F. Kiani, *Sci. Rep.* **2017**, *7*, 9359.
[61] C. F. Buchanan, E. E. Voigt, C. S. Szot, J. W. Freeman, P. P. Vlachos, M. N. Rylander, *Tissue Eng., Part C* **2014**, *20*, 64.
[62] V. L. Silvestri, E. Henriet, R. M. Linville, A. D. Wong, P. C. Searson, A. J. Ewald, *Cancer Res.* **2020**, *80*, 4288.
[63] A. Amann, M. Zwierzina, S. Koeck, G. Gamerith, E. Pechriggl, J. M. Huber, E. Lorenz, J. M. Kelm, W. Hilbe, H. Zwierzina, J. Kern, *Sci. Rep.* **2017**, *7*, 2963.
[64] J. Ko, J. Ahn, S. Kim, Y. Lee, J. Lee, D. Park, N. L. Jeon, *Lab Chip* **2019**, *19*, 2822.
[65] X. Cui, R.-T. T. Morales, W. Qian, H. Wang, J.-P. Gagner, I. Dolgalev, D. Placantonakis, D. Zagzag, L. Cimmino, M. Snuderl, R. H. W. Lam, W. Chen, *Biomaterials* **2018**, *161*, 164.
[66] S. Han, S. Kim, Z. Chen, H. K. Shin, S.-Y. Lee, H. E. Moon, S. H. Paek, S. Park, *IJMS* **2020**, *21*, 2993.
[67] S. J. Hachey, S. Movsesyan, Q. H. Nguyen, G. Burton-Sojo, A. Tankazyan, J. Wu, T. Hoang, D. Zhao, S. Wang, M. M. Hatch, E. Celaya, S. Gomez, G. T. Chen, R. T. Davis, K. Nee, N. Pervolarakis, D. A. Lawson, K. Kessenbrock, A. P. Lee, J. Lowengrub, M. L. Waterman, C. C. W. Hughes, *Lab Chip* **2021**, *21*, 1333.
[68] K. Haase, G. S. Offeddu, M. R. Gillrie, R. D. Kamm, *Adv. Funct. Mater.* **2020**, *30*, 2002444.
[69] T. J. Kwak, E. Lee, *Sci. Rep.* **2020**, *10*, 20142.
[70] E. Wagenblast, M. Soto, S. Gutiérrez-Ángel, C. A. Hartl, A. L. Gable, A. R. Maceli, N. Erard, A. M. Williams, S. Y. Kim, S. Dickopf, J. C. Harrell, A. D. Smith, C. M. Perou, J. E. Wilkinson, G. J. Hannon, S. R. V. Knott, *Nature* **2015**, *520*, 358.
[71] M. B. Chen, J. A. Whisler, J. S. Jeon, R. D. Kamm, *Integr. Biol.* **2013**, *5*, 1262.
[72] C. Hajal, L. Ibrahim, J. C. Serrano, G. S. Offeddu, R. D. Kamm, *Biomaterials* **2021**, *265*, 120470.
[73] S. Azadi, M. Tafazzoli Shadpour, M. E. Warkiani, *Biotechnol. Bioeng.* **2021**, *118*, 823.
[74] S. M. Bhat, V. A. Badiger, S. Vasishta, J. Chakraborty, S. Prasad, S. Ghosh, M. B. Joshi, *J. Cancer Res. Clin. Oncol.* **2021**, *147*, 3477.
[75] M. Shang, R. Hao Soon, C. Teck Lim, B. Luan Khoo, J. Han, *Lab Chip* **2019**, *19*, 369.
[76] J. P. Sleeman, W. Thiele, *Int. J. Cancer* **2009**, *125*, 2747.
[77] E. S. S. Steinskog, S. J. Sagstad, M. Wagner, T. V. Karlsen, N. Yang, C. E. Markhus, S. Yndestad, H. Wiig, H. P. Eikesdal, *Oncotarget* **2016**, *7*, 45789.
[78] N. Frenkel, S. Poghosyan, C. R. Alarcón, S. B. García, K. Queiroz, L. van den Bent, J. Laoukili, I. B. Rinkes, P. Vulto, O. Kranenburg, J. Hagendoorn, *ACS Biomater. Sci. Eng.* **2021**, *7*, 3030.
[79] Y. Cho, K. Na, Y. Jun, J. Won, J. H. Yang, S. Chung, *Front. Bioeng. Biotechnol.* **2021**, *9*, 826.
[80] M. M. Gong, K. M. Lugo-Cintron, B. R. White, S. C. Kerr, P. M. Harari, D. J. Beebe, *Biomaterials* **2019**, *214*, 119225.
[81] P. Fathi, G. Holland, D. Pan, M. B. Esch, *ACS Appl. Biol. Mater.* **2020**, *3*, 6697.
[82] K. M. Lugo-Cintrón, J. M. Ayuso, B. R. White, P. M. Harari, S. M. Ponik, D. J. Beebe, M. M. Gong, M. Virumbrales-Muñoz, *Lab Chip* **2020**, *20*, 1586.
[83] X. Cao, R. Ashfaq, F. Cheng, S. Maharjan, J. Li, G. Ying, S. Hassan, H. Xiao, K. Yue, Y. S. Zhang, *Adv. Funct. Mater.* **2019**, *29*, 1807173.
[84] A. R. Harris, J. X. Yuan, J. M. Munson, *Methods* **2018**, *134–135*, 20.
[85] A. R. Harris, M. J. Perez, J. M. Munson, *BMC Cancer* **2018**, *18*, 718.
[86] A. Nishiguchi, M. Matsusaki, M. R. Kano, H. Nishihara, D. Okano, Y. Asano, H. Shimoda, S. Kishimoto, S. Iwai, M. Akashi, *Biomaterials* **2018**, *179*, 144.
[87] M. Pisano, V. Triacca, K. A. Barbee, M. A. Swartz, *Integr. Biol.* **2015**, *7*, 525.
[88] J. M. Ayuso, M. M. Gong, M. C. Skala, P. M. Harari, D. J. Beebe, *Adv. Healthcare Mater.* **2020**, *9*, 1900925.
[89] N. Schwartz, M. L. S. Chalasani, T. M. Li, Z. Feng, W. D. Shipman, T. T. Lu, *Front. Immunol.* **2019**, *10*, 519.
[90] C. Mondadori, S. Palombella, S. Salehi, G. Talò, R. Visone, M. Rasponi, A. Redaelli, V. Sansone, M. Moretti, S. Lopa, *Biofabrication* **2021**, *13*, 045001.
[91] S. Pérez-Rodríguez, S. A. Huang, C. Borau, J. M. García-Aznar, W. J. Polacheck, *Biomicrofluidics* **2021**, *15*, 054102.
[92] U. Nam, S. Kim, J. Park, J. S. Jeon, *Micromachines* **2020**, *11*, 747.
[93] H. Bosshart, M. Heinzelmann, *Ann. Transl. Med.* **2016**, *4*, 438.
[94] N. Venugopal Menon, H. M. Tay, K. T. Pang, R. Dalan, S. C. Wong, X. Wang, K. H. H. Li, H. W. Hou, *APL Bioeng.* **2018**, *2*, 016103.
[95] W. Lee, S.-K. Ku, J.-S. Bae, *Inflammation* **2015**, *38*, 110.
[96] K. T. Callesen, A. Yuste-Montalvo, L. K. Poulsen, B. M. Jensen, V. Esteban, *Biomedicines* **2021**, *9*, 439.
[97] Y. Xiong, C. C. Brinkman, K. S. Famulski, E. F. Mongodin, C. J. Lord, K. L. Hippen, B. R. Blazar, J. S. Bromberg, *Sci. Rep.* **2017**, *7*, 1633.
[98] D. O. Miteva, J. M. Rutkowski, J. B. Dixon, W. Kilarski, J. D. Shields, M. A. Swartz, *Circ. Res.* **2010**, *106*, 920.
[99] M. Brown, L. A. Johnson, D. A. Leone, P. Majek, K. Vaahtomeri, D. Senfter, N. Bukosza, H. Schachner, G. Asfour, B. Langer, R. Hauschild, K. Parapatics, Y.–K. Hong, K. L. Bennett, R. Kain, M. Detmar, M. Sixt, D. G. Jackson, D. Kerjaschki, *J. Cell Biol.* **2018**, *217*, 2205.
[100] S. Danese, E. Dejana, C. Fiocchi, *J. Immunol.* **2007**, *178*, 6017.

Amanda Bogseth received her Bachelors of Science in Bioengineering from the University of Illinois at Chicago. She is currently a Ph.D. student in the Department of Bioengineering at the University of Maryland. Her research focuses on developing in vitro models of lymphatic vessels to study transport mechanisms in healthy and diseased states.

Ann Ramirez received her Bachelors of Science in Biomedical Engineering from the New Jersey Institute of Technology. She is currently a Ph.D. student in the Department of Bioengineering at the University of Maryland. Her research focuses on exploring the interstitial spaces in lymph nodes to better target therapeutics in healthy and inflamed states.

Erik Vaughan received his Bachelors of Science in Bioengineering from the University of Maryland, College Park. He is currently a Post-Baccalaureate Fellow at the National Institutes of Health. His research focuses on developing in vitro microfluidic models of lymphatic vessels to study drug delivery and transport.

Katharina Maisel is an Assistant Professor in the Fischell Department of Bioengineering at the University of Maryland. She holds a BSE in Materials Science and Engineering from the University of Michigan and a Ph.D. in Biomedical Engineering from The Johns Hopkins University. Her lab uses in vitro modeling, nanotechnology, and immunoengineering approaches to study and develop treatments for diseases at mucosal surfaces with particular emphasis on overcoming biological barriers like mucus and epithelium, and exploring the roles of the lymphatic vasculature and interstitial tissue.